DOKUZ EYLÜL UNIVERSITY

GRADUATE SCHOOL OF NATURAL APPLIED SCIENCES

SYNTHESIS, CHARACTERIZATION AND APPLICATIONS OF pH AND TEMPERATURE SENSITIVE HYDROGELS

by

Aylin ALTINIŞIK

December, 2011

İZMİR

SYNTHESIS, CHARACTERIZATION AND APPLICATIONS OF pH AND TEMPERATURE SENSITIVE HYDROGELS

A Thesis Submitted to the
Graduate School of Natural and Applied Sciences of Dokuz Eylül University
In Partial Fulfillment of the Requirements for the Degree of Doctor of
Philosophy in Chemistry Program

by
Aylin ALTINIŞIK

December, 2011
İZMİR

Ph.D. THESIS EXAMINATION RESULT FORM

We have read the thesis entitled "**SYNTHESIS, CHARACTERIZATION AND APPLICATIONS OF pH AND TEMPERATURE SENSITIVE HYDROGELS**" completed by **AYLİN ALTINIŞIK** under supervision of **PROF. DR. KADİR YURDAKOÇ** and we certify that in our opinion it is fully adequate, in scope and in quality, as a thesis for the degree of Doctor of Philosophy.
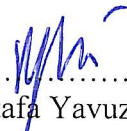
Prof. Dr. Kadir YURDAKOÇ

Supervisor

Prof. Dr. Melek MERDİVAN

Thesis Committee Member

Prof. Dr. Erdal ÇELİK

Thesis Committee Member

Prof. Dr. Erdener KARADAĞ

Examining Committee Member

Prof. Dr. Mustafa Yavuz ERGÜN

Examining Committee Member

Prof. Dr. Mustafa SABUNCU

Director

Graduate School of Natural and Applied Sciences

ii

ACKNOWLEDGMENTS

The author is grateful to the supervisor of this thesis, Prof. Dr. Kadir YURDAKOÇ, for his valuable guide, help and advice, at all stages of this thesis study.

In addition, I wish to express my gratefulness to all friends for their continuous helpful encouragement and valuable supports.

Finally, I would like to thank my family for bringing me in this situation with their unique patience and supports.

Aylin Altınışık

SYNTHESIS, CHARACTERIZATION AND APPLICATIONS OF pH AND TEMPERATURE SENSITIVE HYDROGELS

ABSTRACT

In this study, two different crosslinked Chitosan based hydrogel films were synthesized. In the case of CPT hydrogels, Chitosan was crosslinked with poly(ethylene glycol) (PEG), and tartaric acid, on the other hand, for CVT hydrogels Chitosan was cross-linked with poly(vinyl alcohol) (PVA) and tartaric acid (TA). The synthesized hydrogel films were characterized using FTIR, NMR, XRD and SEM analysis. The TGA / DTG and DSC analysis were also made for the determination of thermal properties of hydrogel films. Swelling properties of these hydrogel films were investigated at two different pHs (1.2 and 7.4) and temperatures (4 and 37 °C). At the same time, reversible swelling and de-swelling behavior of these samples were investigated at specific temperature and pH. The swelling behaviors of all samples were increased in acidic medium, while decreased in basic medium. Similarly, the degree of swelling of hydrogels was decreased with the increase in the amount of PEG and PVA. It has been observed that swelling of PEG containing CPT hydrogels in acidic medium and deswelling of these hydrogels in basic medium were much more than for PVA containing CVT hydrogels. At the temperatures changes, while all of the samples were more swollen at 37 °C, they were less swollen at 4 °C. Also both of the hydrogels were investigated for the enzymatic degradation with lysozyme. The tendency of the enzymatic degradation rates was found to be parallel with the swelling ratio for CPT hydrogel. On the other hand, degradation of CPT Hydrogels in lysozyme, were faster than pure Chitosan film. However, in the case of CVT hydrogel, the opposite result was observed due to the different crystalline form and degradation of CVT hydrogel which was slower than pure Chitosan hydrogel films. In addition, all of the hydrogels were used for application which is drug release system. In the experiments, KCl/HCl and PBS buffer solution were used for the artificial stomach environment and intestinal environment, respectively as a release medium. Also, amoxicillin were used as a model drug for release study. All of the amoxicillin in the samples were released at the artificial stomach environment. On the other hand, they were partly released the

amoxicillin in the artificial intestinal environment. At CPT hydrogel films, increasing of amount of PEG was observed in the case of decreasing of release rate and amount of drug. Similar swelling behaviors were also observed in CVT hydrogel films. However, drug release behaviors of CVT hydrogel films were slower and can be controlled as compared with CPT. In artificial intestinal environment, the drug release rates of amoxicillin on CPT hydrogel films were faster than on CVT hydrogel films, and CVT hydrogel films may be more appropriate for controlled release of amoxicillin.

Keywords: Chitosan, responsive hydrogel, biodegradation, drug delivery.

pH VE SICAKLIK DUYARLI HİDROJELLERİN SENTEZİ, KARAKTERİZASYONU VE UYGULAMALARI

ÖZ

Bu çalışmada kitosan tabanlı iki farklı çapraz bağlı hidrojel film sentezlenmiştir. Bunlardan ilki poli(etilen glikol) (PEG) ve tartarik asitle çapraz bağlanırken ikincisi poli(vinil alkol) (PVA) ve tartarik asitle çapraz bağlanmıştır. Sentezlenen hidrojel filmleri FTIR, NMR XRD ve SEM analizleri kullanılarak karakterize edilmiştir. Termal özelliklerin belirlenmesi için ise TGA/DTG ve DSC analizleri yapılmıştır. Bu hidrojel filmlerin iki farklı pH (1,2 ve 7,4) ve sıcaklık (4 ve 37 °C) ortamında şişme özellikleri incelenmiştir. Aynı zamanda tüm örneklerin belirtilen pH ve sıcaklıklarda tekrarlanabilir şişme ve büzüşme davranışları incelenmiştir. Tüm örneklerin şişme davranışları asidik ortamda artmasına rağmen, bazik ortamda azalmaktadır. Benzer şekilde hidrojeller içindeki PEG ve PVA miktarının artışı ile şişme derecesinin azaldığı görülmektedir. PEG içeren CPT hidrojellerin asidik ortamdaki şişmesi ve bazik ortamdaki büzüşmesi, PVA içeren CVT hidrojeline göre çok daha fazla olduğu gözlenmiştir. Sıcaklık farklanmasında ise tüm örneklerin yüksek sıcaklıkta daha fazla şişerken düşük sıcaklıkta daha az şiştiği gözlenmiştir. Ayrıca, her iki hidrojelin lizozimle enzimatik bozunması incelenmiştir. CPT hidrojelleri için, enzimatik bozunma eğilim şişme oranları ile paralel bulunmuştur. Diğer yandan, CPT hidrojelinin lizozim içindeki bozunma hızı saf kitosan hidrojelinkinden daha hızlıdır. CVT hidrojelinde ise, tam tersi sonuç gözlenmiştir. Bu durum, CVT hidrojelinin farklı kristal yapısından dolayı saf kitosandan daha yavaş bozunmasından ileri gelmektedir.

Buna ek olarak, tüm hidrojeller, ilaç salım sistemi uygulamalarında kullanılmıştır. Bu çalışmada model ilaç olarak amoksisilin kullanılmıştır. Salınım ortamı için yapay mide ortamı olarak KCl/HCl tamponu ve bağırsak ortamı için PBS tamponu kullanılmıştır. Tüm örnekler yapay mide ortamında salınım yaparken yapay bağırsak ortamında kısmen salınım yapmaktadır. Yapay mide ortamındaki CPT hidrojel filmlerinde PEG miktarının artmasıyla salınım hızının ve ilaç miktarının azaldığı görülmektedir. Benzer sonuç CVT hidrojel filmlerinde de gözlenmiştir. Ancak CPT ve CVT hidrojel filmleri karşılaştırıldığında PVA içeren CVT hidrojellerinin ilaç

salınımının daha yavaş ve kontrol edilebilir olduğu gözlenmiştir. Yapay bağırsak ortamında ise, PEG içeren CPT hidrojellerinin salınımın PVA içeren CVT hidrojellerine göre daha hızlı olduğu ve CVT hidrojellerinin kontrollü salınım için daha uygun olduğu gözlenmiştir.

Anahtar Kelimeler: Kitosan, akıllı hidrojel, biyobozunurluk, ilaç taşınımı

CONTENTS **Page**

CHAPTER ONE
INTRODUCTION

1.1 Hydrogels

Hydrogels are comprised of cross-linked polymer networks that have a high number of hydrophilic groups or domains. These networks have a high affinity for water, but are prevented from dissolving due to the chemical or physical bonds formed between the polymer chains. Water penetrates these networks causing swelling, giving the hydrogel its form (Bhattarai, Gunn, & Zhang, 2010). Hydrogels are water swollen polymer matrices, with a tendency to imbibe water when placed in aqueous environment. They swell considerably in an aqueous medium and demonstrate extraordinary capacity (>20%) for imbibing water into the network structure.

1.2 General Definitions

Gels exhibiting a phase transition in response to change in external conditions such as pH, ionic strength, temperature and electric currents are known as "stimuli-responsive" or "smart" gels.
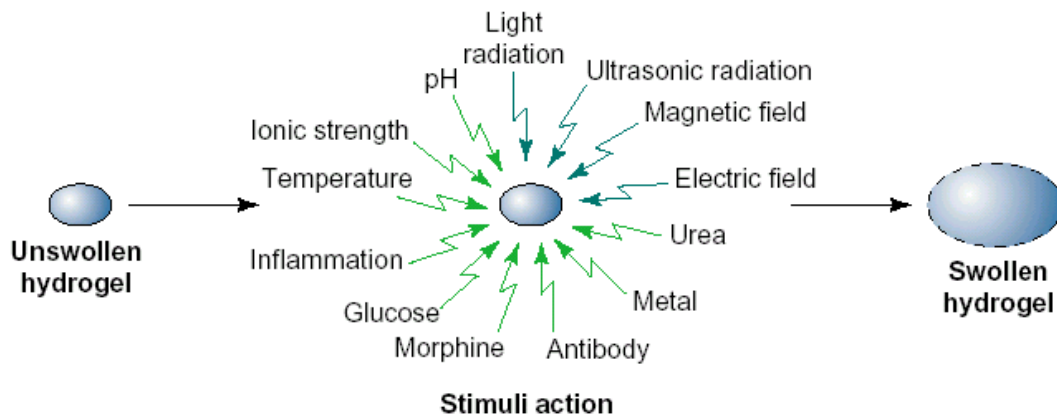
Figure 1.1 Responsive Hydrogels (Gupta, Vermani, & Garg, 2002).

Being insoluble, these three-dimensional hydrophilic networks can retain a large amount of water that not only contributes to their good blood compatibility but also maintains a certain degree of structural integrity and elasticity. Hydrophilic

functional groups such as –OH, –COOH, –CONH$_2$, and –SO$_3$H present in the hydrogel are capable of absorbing water without undergoing dissolution.

Hydrogels can be prepared from natural or synthetic polymers. Although hydrogels made from natural polymers may not provide sufficient mechanical strength and may contain pathogens or evoke immune/inflammatory responses, they do offer several advantageous properties such as inherent biocompatibility, biodegradability and biologically recognizable moieties that support cellular activities. Synthetic hydrogels, on the other hand, do not possess these inherent bioactive properties. Fortunately, synthetic polymers usually have well-defined structures that can be modified to yield tailored degradability and functionality (Bajpai, Sandeep, Smitha & Sanjana 2008).
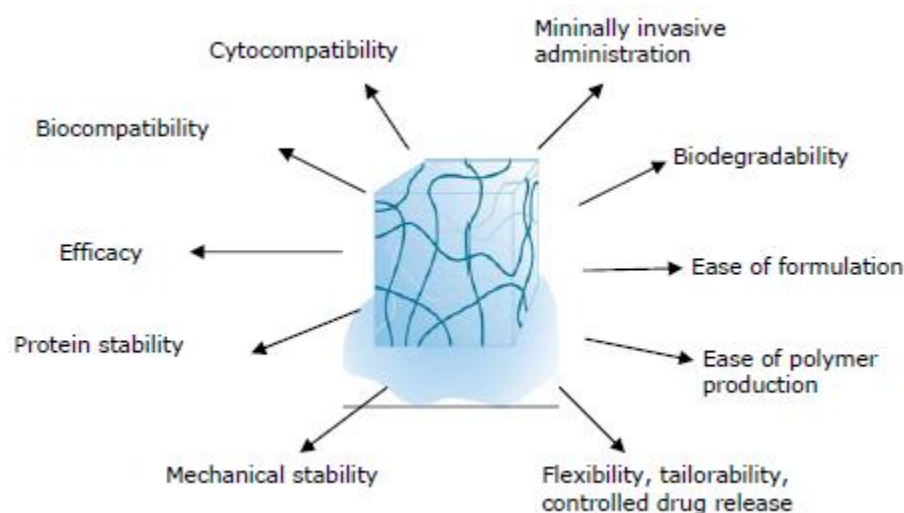
Figure 1.2 Overview of the ideal characteristics of a hydrogel for biomedical and pharmaceutical applications (Censi, 2010).

1.3 Classifications of Hydrogels

Hydrogels can be classified as neutral or ionic, based on the nature of side groups. In neutral hydrogels, the driving force for swelling is due to the water-polymer thermodynamic mixing contribution to the overall free energy, along with elastic polymer contribution (Peppas, Bures, Leobandung, & Ichikawa, 2000). The swelling of ionic hydrogels is also affected by the ionic interactions between charged

polymers and free ions (Peppas, & Khare, 1993). Ionic hydrogels containing ionic groups, such as carboxylic acid, imbibe larger amount of water, because of its increased hydrophilicity. Examples of such gels are poly (acrylic acid), and polyamines. Hydrogels are also classified as homopolymers or copolymers, based on the method of preparation. Hydrogels can be classified based on the physical structure of the network as amorphous, semi-crystalline, hydrogen bonded structures, supermolecular structures and hydrocolloidal aggregates (Peppas, Bures, Leobandung, & Ichikawa, 2000). Important classes of hydrogels are the stimuli responsive gels (Ji, Mourad, Fried & Dolbow, 2006). These gels show swelling behavior dependent on their physical environment. These gels can swell, or deswell in response to changes in pH, temperature, ionic strength, and electromagnetic radiation (George & Abraham, 2007). These properties allow for usage in a number of applications, such as separation membranes, biosensors, artificial muscles, and drug delivery devices (Lin & Metters, 2006).

1.3.1 Stimuli Responsive Hydrogels

Hydrogels have been developed as stimuli-responsive materials, which can undergo abrupt volume change in response to small changes in environmental parameters: temperature, pH, ionic strength, etc. (Figure 1.1). These unique characteristics of hydrogels are of great interest in drug delivery, cell encapsulation and tissue engineering (Plunkett, Berkowski, & Moore, 2005; Schilli, Zhang, rizzardo,Thang, Chong, & Edwards, 2004). Stimuli-responsive hydrogels play an important role in the development of novel smart hydrogels (Zhang, Yang, Chung, & Ma, 2001). The most important systems from a biomedical point of view are those sensitive to temperature and/or pH of the surroundings. The human body exhibits variations of pH along the gastrointestinal tract, and also in some specific areas like certain tissues (and tumoral areas) and subcellular compartments. Polymer–polymer and polymer–solvent interactions show an abrupt readjustment in small ranges of pH or temperature. In the case of pH sensitive polymers, the key element of the system is the presence of ionizable weak acidic or basic moieties attached to a hydrophobic backbone. Upon ionization, the coiled chains extend dramatically, responding to the electrostatic repulsions of the generated charges (anions or cations).

Stimuli-responsive sensitive polymer gels offer potential economic alternatives to conventional separation processes for industrial applications (Kucuk, & Kuyulu, 2005). Controlled permeability variations of responsive gels have also been used to achieve a variety of size- or charge-selective separations. In addition to pH and temperature, other stimuli-responsive hydrogels have been produced that exhibit dramatic changes in their swelling behavior, network structure, permeability and mechanical strength in response to a number of external stimuli, including the presence of specific solutes and applied electrical or magnetic fields (Shiga, Hirose, Okada, & Kurauchi, 1992).

Another novel type of responsive polymers results from surface modification of a polymer matrix by attachment of responsive chains to produce responsive interfaces showing different behavior in response to small changes in environmental parameters. Surfaces may change from hydrophobic to hydrophilic (Uhlmann, Houbenov, Stamm, & Minko, 2005) or show a variation in pore size (Geismann, & Ulbricht, 2005).

1.3.1.1 pH-Responsive Hydrogels

pH sensitive polymers are normally produced by adding acidic or basic functional groups to the polymer backbone; these either accept or release protons in response to appropriate pH and ionic strength changes in aqueous media (Langer R, & Peppas, 2003). The network porosity of these hydrogels changes with electrostatic repulsion. Ionic hydrogels containing carboxylic or sulfonic acid groups show either sudden or gradual changes in their dynamic or equilibrium swelling behavior as a result of changing the external pH. The degree of ionization of these hydrogels depends on the number of acidic groups in the hydrogel, which results in increased electrostatic repulsions between negatively charged carboxyl groups on different chains. This, in turn, results in increased hydrophilicity of the network and greater swelling ratio at high pH. Conversely, hydrogels containing basic groups, such as amines, ionize and show electrostatic repulsion at low pH (Zhang, Tang, Bowyer, Eisenthal, & Hubble. 2005).
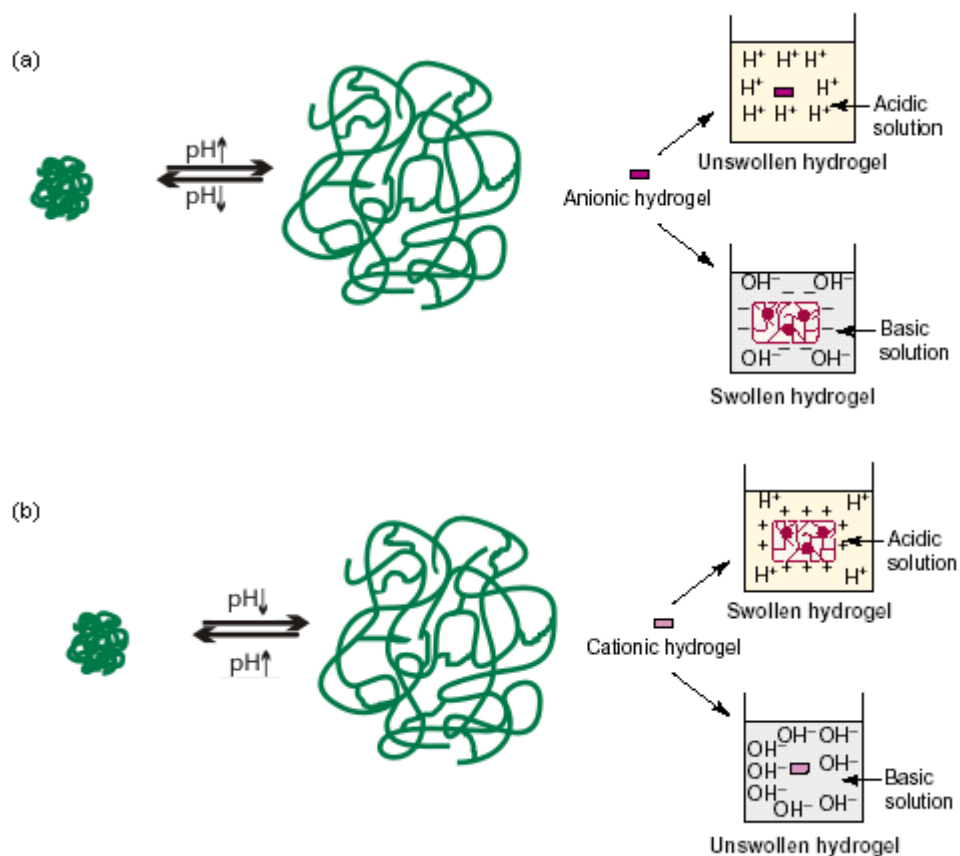
Figure 1.3 The pH-responsive swelling of **(a)** anionic and **(b)** cationic hydrogels (Gupta, Vermani, & Garg, 2002).

1.3.1.2 Temperature-Responsive Hydrogel

Thermosensitive polymers, like pH responsive systems, offer many possibilities in biomedicine. They present a fine hydrophobic–hydrophilic balance in their structure; and small temperature changes around a critical solution temperature (CST) make the chains collapse or extend, responding to adjustments of the hydrophobic and hydrophilic interactions between the polymer chains and the aqueous medium (Ebara, Yamato, Hirose, Aoyagi, Kikuchi, & Sakai, 2003; Schmoljohann, Oswald, Jorgensen, Beyerlein, &Werner, 2003; Liu, Yang, Liu & Tong, 2003). A critical solution temperature may be defined as a temperature at which the polymer solution undergoes separation from one phase to two phases. Thus, temperature sensitive polymers undergo an abrupt change in volume as the temperature of the medium is varied above or below the CST (Xu, Kang, & Neoh, 2006). These unique

characteristics make hydrogels especially useful in biomedical applications such as controlled release of drugs and in tissue engineering (Wu, Liu, Heng, & Yang, 2005; Zangh, Lewis, & Chu, 2005; Christopher & Peppas, 1996).
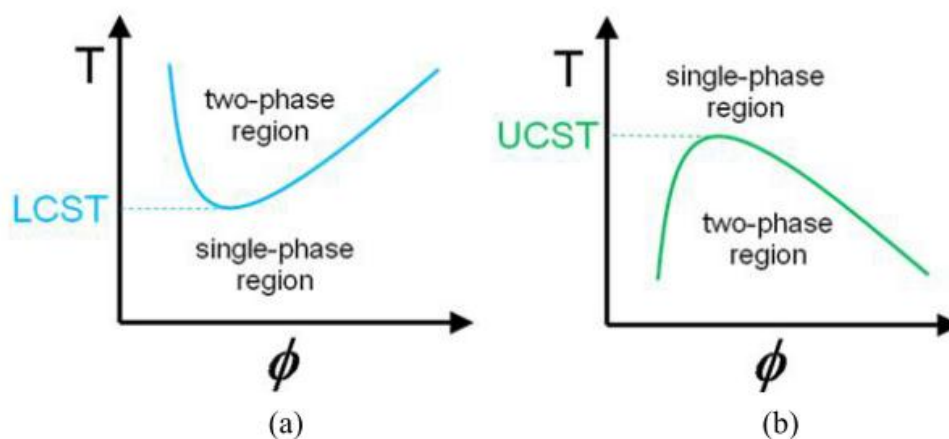
Figure 1.4 Temperature vs. polymer volume fraction, ϕ. Schematic illustration of phase diagrams for polymer solution (a) lower critical solution temperature (LCST) behavior and (b) upper critical solution temperature (UCST) behavior (Ward & Georgiou, 2011).

1.4 Applications of Hydrogels

Hydrogels, crosslinked hydrophilic polymers, represent an important class of biomaterials in biotechnology and medicine because many hydrogels exhibit excellent biocompatibility, causing minimal inflammatory responses, thrombosis, and tissue damage (Graham, 1998). Hydrogels can also swell large quantities of water without the dissolution of the polymer due to their hydrophilic but crosslinked structure, thus giving them physical characteristics similar to soft tissues. In addition, hydrogels have high permeability for oxygen, nutrients, and other water-soluble metabolites. Over the past three decades, a number of hydrogels differing in structure, composition, and properties have been developed. Hydrogel materials have been used extensively in medicine for applications such as contact lenses, biosensors, linings for artificial implants (Peppas, Bures, Leobandung & Ichikawa; 2000).

1.4.1 Pharmaceutical Applications

Much of the research on hydrogels has been focused on the application in controlled drug delivery (Peppas, 1987). While zero-order drug release is important for most drugs, there are many drugs that need to be delivered in a pulsatile fashion. The most widely used example is the delivery of insulin. Temporal control of insulin delivery can be achieved by utilization of smart hydrogels which release more insulin in response to increase in glucose level. Most glucose-responsive hydrogel systems are made of pH-sensitive polymers such as poly(diethylaminoethyl methacrylate) (PDEAEMA) (Park, & Park; 1996) and glucose oxidase, which transforms glucose into gluconic acid. In addition to the pH-responsive hydrogels, the glucose-sensitive dissolvable hydrogels have been used to control the insulin release. Microspherical hydrogels such as alginate microparticles have been used to encapsulate insulin producing cells for the delivery of insulin (Park, & Park; 1996). Pulsatile delivery of drugs can also be achieved by temperature-responsive hydrogels. Thermo-sensitive hydrogels are usually made of polyacrylamide derivatives with hydrophobic groups which promote hydrophobic interactions necessary for shrinking at elevated temperatures. The volume collapse temperature can be adjusted by varying the hydrophobic groups (Park, & Park; 1996).

1.4.1.1 Drug Release

Drug release generally involves simultaneous absorption of water and desorption of drug via a swelling-controlled mechanism (Rao & Devi, 1988). The rate-controlling factor mediating drug delivery is the resistance of the polymer to an increase in volume and change in shape (Bouwstra & Junginger, 1993).

A glassy hydrogel, on coming into contact with water or any other thermodynamically compatible medium allows solvent penetration into free spaces on the surface between the macromolecular chains. When enough water has entered the matrix, the glass transition temperature of the polymer drops to the experimental temperature. The presence of solvent in a glassy polymer causes the development of stresses that are accommodated by an increase in the radius of gyration and end-to-

end distance of polymer molecules, which is seen macroscopically as swelling (Gupta et al., 2002).

Controlled drug delivery applications include both sustained (over days /weeks/months/years) delivery and targeted (e.g. to a tumor, diseased blood vessel, etc.) delivery on a one-time or sustained basis. Although the field of controlled drug delivery encompasses a wide range of drugs, two key factors which stimulated the emergence of the field are the rise of proteins as potential pharmaceuticals and the demonstration that sustained release of active proteins macro-molecules rather than small polymer-permeable drugs from polymer matrices was possible.

There are two general methods for loading of hydrogels as drug carriers. In one method, the hydrogel monomer is mixed with drug, an initiator, with or without a cross-linker, and allowed to polymerize, trapping the drug within the matrix (Song, 1981). In the second approach, a preformed hydrogel is allowed to swell to equilibrium in a suitable drug solution. The drug loaded hydrogel is dried and device is obtained. The latter method has some advantages over the first method because polymerization conditions may have deleterious effects on drug properties and the difficulties in device purification after loading and polymerization often remain (Kim, Boe & Okano, 1992).

1.4.1.1.1 The Model Drug Amoxicillin and Its Properties. Amoxicillin belongs to the penicillin class of antibiotics. Amoxicillin is a moderate-spectrum, bacteriolytic, β-lactam antibiotic used to treat bacterial infections caused by susceptible microorganisms. Amoxicillin is effective against many different bacteria including Haemophilus influenza, Neisseria gonorrhea, Escherichia coli, Pneumococci, Streptococci, and certain strains of Staphylococci. It is usually the drug of choice within the class because it is better absorbed, following oral administration, than other b-lactam antibiotics. It acts by inhibiting the synthesis of bacterial cell wall, which protects bacteria from their environment. (Bebu, Leopold, Berindean & David; 2011)

Amoxicillin is an efficient antibiotic drug for the treatment of Helicobacter pylori, the main cause of gastritis and stomach ulcer. Helicobacter pylori are a parasite that resides underneath the mucous membrane of the stomach, avoiding attack by strong

acid, which no bacteria can survive. It eventually leads to continual degeneration of the stomach mucous membrane by secretion of a urea-degradable enzyme (Bardonnet, Faivre, Pugh, Piffaretti & Falson; 2006). About 40% of the population is reported to be infected by this bacterium, with approx. 10% of those suffering from a resulting digestion ulcer. A pro-drug is a drug administered into the body that is subsequently transformed into a slightly different chemical structure from its original. It is re-converted to an active drug by hydrolysis or enzyme reaction inside the body. The pro-drug can enhance curing efficiency because it reaches the target locations at a very high concentration without any degradation (Greenwald, Gilbert, Pendri, Conover, Xia & Martinez; 1996). Amoxicillin has been loaded in and released from several polymeric delivery systems for its site-specific delivery in the stomach. One of them involves polyionic complexes of Chitosan and polyacrylic acid. The release of amoxicillin accompanied by the swelling of the polymeric system is mainly governed by the degree of ionization (Torre, 2003). Amoxicillin mucoadhesive microspheres containing mucoadhesive Chitosan (Patel, 2007) or carboxyl vinyl polymer (Patel, 2009; Nagahara, 1998), and Chitosan–poly (acrylic acid) (Yadav, Satish & Shivakumar; 2007), poly (acrylic acid)–poly (vinyl pyrollidone) complexes (Chun, Sah & Choi, 2005) have been prepared. The drug-release pattern was mostly controlled by the mucoadhesive properties of the microspheres on the gastric mucous layer (Patel & Patel, 2007; Chun et al., 2005). In order to establish a prolonged release of a drug in the stomach, a long retention time of the drug carrier is a prerequisite. To accomplish this long retention time, high and fast swelling properties of the drug carrier in acidic conditions are required for its stable suspension. These swelling properties of the drug-carrying tablet prevent it from escaping the stomach through the pylori (diameter approx.1.3 cm) (Bardonnet et al., 2006). One of the promising materials to attain this sustained release is a super porous hydrogel that can absorb high levels of water in a short time to expand its volume considerably without dissolution by the presence of large pores in a 3-dimensional network structure.

Figure 1.5 Structure of amoxicillin

1.4.2 Biomedical Applications

The applications of hydrogels in biomedical fields are diverse ranging from diagnostic device to artificial muscle. Application of hydrogels as contact lenses and intraocular lenses has a rather long history compared with other applications. Soft contact lenses made of hydrogels possess desirable properties such as high oxygen permeability, although they have problems of protein deposits and lens spoliation. Soft intraocular lenses have advantages over rigid types. Their ability to be folded allows surgeon to use a much smaller surgical incision (Park & Park, 1996). The hydrogel contact and intraocular lenses can be sterilized by autoclaving, which is more convenient than the sterilization by ethylene oxide needed for rigid lenses made of poly(methyl methacrylate).

Hydrogels are commonly used as wound dressing materials, since they are flexible, durable, non-antigenic, and permeable to water vapor and metabolites, while securely covering the wound to prevent bacterial infection. Methylcellulose hydrogel has been used to deliver allergens in skin testing. When test allergens are delivered in the hydrogel vehicle, less skin irritation was observed.

Hydrogels are also often coated on the urinary catheter surface to improve its biocompatibility (Park et. al; 1996). The hydrogel layer not only provide smooth, slippery surface, but also it can prevent bacterial colonization on the surface. Hydrogel layers formed on the inner surface of injured arteries are known to reduce thrombosis and intimai thickening in animal models. Intimai thickening was

prevented by inhibiting contact between blood and subendothelial tissue with a hydrogel layer. The swelling pressure of p(HEMA) hydrogel was used to stabilize the bone implants. With improved design of the implant, such hydrogels are expected to be effectively used as a stabilizing interface.

The potential applications of hydrogels in sterilization and cervical dilatation have been explored. When a hydrogel which forms in situ plug was placed into fallopian tubes of rabbits by transcervical catheterization, conception was prevented. With more structurally rigid and biocompatible hydrogels the tubular sterilization system can be developed. Hydrogel rods were developed to deliver hormones such as prostaglandin analogs as well as to mechanically dilate the cervix. Dilatation of the cervical canal is necessary for the first trimester-induced abortion by suction curettage. One of the advanced applications of hydrogels is in the development of artificial muscles. Smart hydrogels which can transform electrochemical stimuli into mechanical work (i.e., contraction) can function like the human muscle tissue. Polymeric gels capable of reversible contraction and expansion under physicochemical stimuli are essential in the development of advanced robotics with electrically driven muscle-like actuators. Smart materials that emulate the contractions and secretions of human organs in response to changes in environmental conditions such as temperature, pH, or electric field may soon find a use in medical implants, prosthetic muscles or organs, and robotic grippers (Park et. al., 1996).

1.5 Materials Used for The Synthesis of The Hydrogels

1.5.1 Chitosan and Its Properties

Chitosan (2-amino-2deoxy-(1→4)-β-D-glucopyranan), a polyaminosaccharide, normally obtained by alkaline deacetylation of chitin is the principal component of living organisms such as fungi and crustacean (Figure 1.6). When its DA (degree of N- acetylation) is lower than 50%, the chitin becomes soluble in aqueous acidic solution and is named Chitosan. Up to the present time only a few cationic polymers exist and Chitosan may be used as a flocculation and chelating polymer (Dung, Milas, Rinaudo, & Desbrieres; 1994).
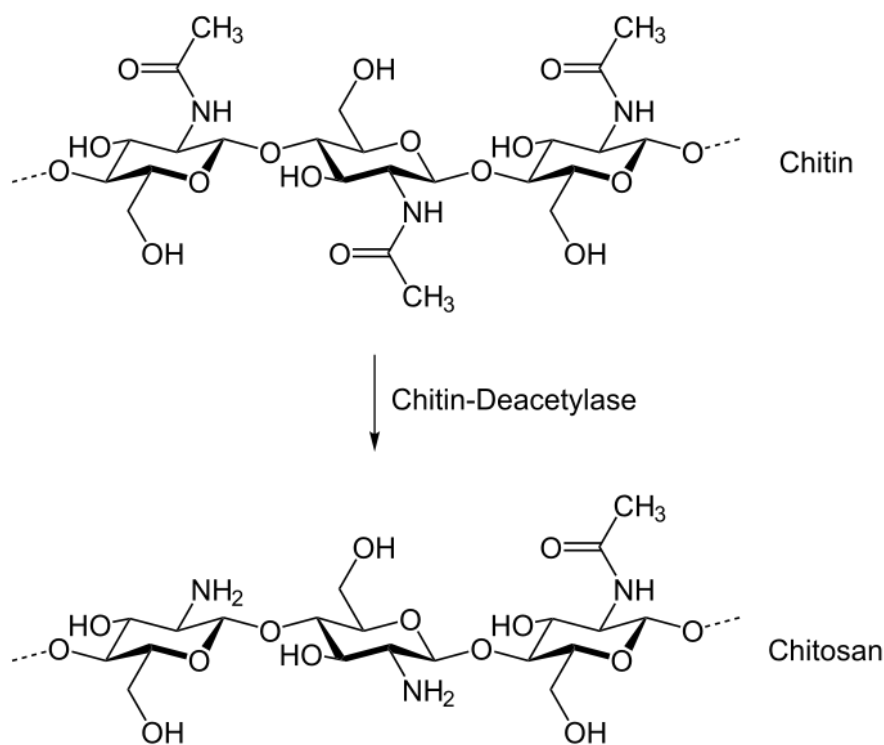
Figure 1.6 Synthesis of Chitosan from chitin

Chitosan a linear polymer of mainly anhydroglucosamine which behaves as a linear polyelectrolyte at acidic pH is nontoxic and bioabsorbable. At pH below 6.5, Chitosan in solution carries a high positive charge density, one charge per glucosamine unit. Since Chitosan is one of the few cationic polyelectrolytes, it is an exception to the current industrial high molecular weight polysaccharides, which are mostly neutral or polyanionic. It was documented that oral administration of Chitosan with drugs enhanced their absorption from intestines into blood in animals. Chitosan is being evaluated in a number of biomedical applications including wound healing and dressing, dialysis membranes, contact lenses, fibers for digestible sutures, liposome stabilization agents, antitumor uses and drug delivery uses and controlled-release systems. In these uses Chitosan's key properties are 1) biocompatibility, 2) nonantigenicity, 3) nontoxicity, (its degradation products are known natural metabolites), 4) the ability to improve wound healing/or clot blood 5) the ability to absorb liquids and to form protective films and coatings, and 6) selective binding of acidic liquids, thereby lowering serum cholesterol levels. But Chitosan has some drawbacks, it is only soluble in aqueous medium in the presence

of a small amount of acid such as acetic acid and its mechanical properties are not good for some biomedical application. Therefore many researchers tried to modify its properties.

1.5.2 Poly(ethylene glycol) and Its Properties

Poly(ethylene glycol) (PEG), otherwise known as poly(oxyethylene) or poly(ethylene oxide) (PEO), is a synthetic polyether that is readily available in a range of molecular weights. Materials with M_w <100,000 are usually called PEGs, while higher molecular weight polymers are classified as PEOs. These polymers are amphiphilic and soluble in water as well as in many organic solvents (e.g., methylene chloride, ethanol, toluene, acetone, and chloroform). Low molecular weight (M_w <1,000) PEGs are viscous and colorless liquids, while higher molecular weight PEGs are waxy, white solids with melting points proportional to their molecular weights to an upper limit of about 67 °C (Bailey, & Koleske, 1976).

PEG is a faculty of water soluble polymers with many different molecular weights that exhibits useful properties such as protein resistance, low toxicity and immunogenicity. PEGs have frequently been chosen as drug carriers due to biocompatibility and minimal toxicity and good solubility in water or other common solvents. PEGs have frequently been co-polymerized with linear aliphatic polyesters like poly(lactic acid) for use in drug delivery systems and tissue engineering and also for improving the biocompatibility. Because of the good biological activities of Chitosan and PEG, a combination of Chitosan and PEG may have beneficial effects on the biological characteristics of complex membranes. The major advantages of this approach are its simplicity, low cost and improved mechanical properties and biocompatibility. In the last few decades many different types of per oral controlled release (CR) formulations have been developed to improve clinical efficacy of the drug and patient compliance. These formulations are designed to deliver the drugs at a controlled and predetermined rate, thus maintaining their therapeutically effective concentrations in systems in systemic circulation for prolonged periods of time. In-vivo performance of these dosage forms depends greatly on their physical and

structural properties, and consequently on their drug release mechanisms and its kinetics (Sood & Panchagnula, 1998).

It is known that hydrophilic monomers provide a distinct advantage in both fabrication and application of hydrogels. The premier material used today for both drug delivery, cell encapsulation and as adhesion promoters is Poly (ethylene glycol) hydrogels. PEG has many unique properties which make it an ideal choice. PEG and its "stealth " properties, that is once its attached to certain formulations, it allows slow release of the formulation, thus enabling controlled release, as well as reduce uptake of harmful immunoglobins. This allows longer dosage and reduces immunogenicity of substances such as adenosine deaminase (ADA) and asparaginase (Russell, et al., 2001). PEG is nontoxic, thus ideal for biological applications, and can be injected into the body without adverse effects. It is also an FDA approved materials for use in humans. PEGylation is an important technique being developed for drug delivery, involves attachment of PEG to proteins and drugs, and has great potential for improving pharmokinetic and pharmodynamic properties of delivered drugs. Thus PEG has varied uses in the medical field, including drug delivery (e.g.; treatment of hepatitis C), laxatives, cell immobilization, (as adhesion promoters), biosensor materials, and encapsulation of islets of langerhans for treatment of diabetes. It is also used as carrier material for encapsulated cells for tissue engineering purposes. Thus PEG, with its biocompatibility, flexibility and stealth properties is an ideal material for use in pharmaceutical applications.

PEG has several chemical properties that make it especially useful in various biological, chemical and pharmaceutical settings:

- Non-toxic and non-immunogenic – can be added to media and attached to surfaces and conjugated to molecules without interfering with cellular functions or target immunogenicities,
- Hydrophilic (aqueous-soluble) – attachment to proteins and other biomolecules decreases aggregation and increases solubility,
- Highly flexible – provides for surface treatment or bioconjugation without steric hindrance.

1.5.3 Poly (vinyl alcohol) and Its Properties

Poly(vinyl alcohol) (PVA) is a water-soluble polyhydroxy polymer, employed in practical applications because of its easy preparation, excellent chemical resistance and physical properties, and because it is completely biodegradable (Park, & Ruckenstein, 2001). Although PVA has good mechanical properties in the dry state, its high hydrophilicity limits its applications (Park, et al., 2001; Hodge, Edward, & Simon, 1996; Muhlebach, Muller, Pharisa, Hofmann, Seiferling, & Guerry, 1997). PVA can generate a physical hydrogel by freeze–thaw cycles and a chemical hydrogel by the chemical reaction of its hydroxyls with a crosslinker. It can also form hydrogels through its complexation with inorganic ions, such as the borate ions (Gimenez, Reina, Mantecon, & Cadiz, 1999). PVA was chemically modified by using aldehydes, carboxylic acids, anhydrides, and thus its hydrophilicity, thermal and mechanical properties could be modified. The chemically crosslinked PVA hydrogels have received increasing attention in biomedical and biochemical applications, because of their permeability, biocompatibility and biodegradability (Park, et al., 2001).

PVA has excellent film forming, emulsifying, and adhesive properties. It is also resistant to oil, grease and many solvent. It is odorless and nontoxic. It has high tensile strength and flexibility, as well as high oxygen and aroma barrier properties. However these properties are dependent on humidity, in other words, with higher humidity more water is absorbed. The water, which acts as a plasticizer, will then reduce its tensile strength, but increase its elongation and tear strength. PVA is fully degradable and is a quick dissolver. PVA has a melting point of 230°C and 180–190°C for the fully hydrolyzed and partially hydrolyzed grades, respectively. It decomposes rapidly above 200°C as it can undergo pyrolysis at high temperatures.

PVA is an atactic material but exhibits crystallinity as the hydroxyl groups are small enough to fit into the lattice without disrupting it. PVA is close to incompressible.

1.5.4 Tartaric Acid and Its Properties

Tartaric acid is a diprotic organic acid that can be found in many plants like bananas, grapes, and tamarinds. The most prevalent use of tartaric acid is in the making of wine. Tartaric acid adds to the tart flavor of wine, and causes the crystals that are sometimes called wine diamonds on the cork. Tartaric acid comes in many different forms, including levotartaric acid, dextrotartaric acid, mesotartaric acid, and racemic acid. Tartaric acid can be a toxin to the muscular system, and its level in the body may be elevated in those with muscular diseases.

- Physical Properties

Tartaric acid appears as small white crystals when it is in its solid form. There is no odor to tartaric acid, but inhalation may cause coughing and sneezing. The solid form melts at 206°C. Tartaric acid can be used to create several different salts, including cream of tartar, tartar emetic, and Rochelle salt. When added to water, cream of tartar cleans copper coins, which is not surprising considering that tartaric acid is used in some laboratory copper oxide reactions.

- Chemical Properties

Some of the names for tartaric acid used in chemistry include 2,3-dihydroxysuccinic acid, uvic acid, and paratartaric acid. The basic molecular formula for the acid is $C_4H_6O_6$. The molar mass of the acid is 150.087 grams per mole. An interesting chemical property of tartaric acid is that it is chiral, which means its molecules are not super imposable on their mirror-images. This property gives it the ability to rotate polarized light. This light rotation does not occur in one form of tartaric acid called DL-tartaric acid. A large amount of tartaric acid (around 500 grams) would be lethal to a human being.

- Structural Properties

Levotartaric acid (D-(−)-tartaric acid)   Dextrotartaric acid (L-(+)-tartaric acid)
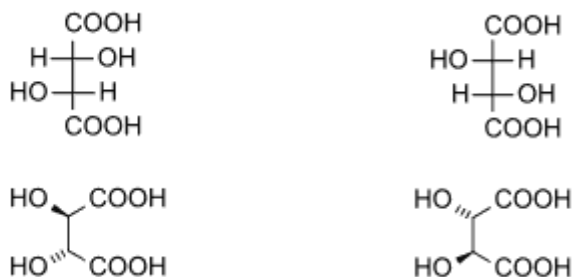
The structural formula of tartaric acid is $HO_2CCH(OH)CH(OH)CO_2H$. A molecule of the acid has two acids groups and two alcohol groups. The second and third carbon groups are asymmetrical, which leads the molecule to be chiral. The different forms of the acid have slightly different structures, which causes light to be rotated a different direction or not at all. L-tartaric acid is the structure that is most practically usable in the chemical field (Properties of Tartaric Acid, http://www.ehow.com/list_6388695_properties-tartaric-acid.html)

1.6 Aim of The Study

So far there are lots of synthesized chitosan based hydrogel in the literature. But, toxic crosslinker were used in virtually all of the synthesized hydrogels. Applications of hydrogels which were synthesized by using toxic crosslinker are narrowed. At the same time biodegradability of hydrogel is damaged with the usage of toxic crosslinker.

In this study, firstly, we aimed to synthesis chitosan based hydrogel by using a non toxic crosslinking agent. Also, we targeted to be biodegrable hydrogels. And then, synthesized hydrogels will be characterized with Fourier transformed infrared (FTIR), nuclear magnetic resonance (NMR) for investigate the formation of the crosslinked structure. Thermal properties will be investigated with thermo gravimetric analysis (TGA/DTG) and differential scanning calorimetry (DSC).

Secondly, we hope to produce pH and temperature sensitive materials for used drug delivery system, because controlled release system aims at delivering the right drug at the right place, at right concentration for the right period of time. Sometimes direct delivery of such drugs is difficult, due to the discomfort caused to the patient. For such cases, strategies have been developed for delivering drug with a carrier. The

drug carrier whether it be an implantable device or long chain polymer must be biocompatible with the drug and the body. Drug delivery systems alter the biodistribution and pharmokinetics of the drug. Therefore some obstacles must take into such as drug solubility, enzyme degradation, toxicity, inability to cross biological barriers as well as adverse environmental conditions. In order to make the delivery of the drug effective without causing an immune response in the body, proper design and engineering of the drug delivery system is essential.

Localized drug delivery can be achieved by introducing the drug directly at the target site. The major class of biomaterials considered as implantable drug delivery systems are hydrogels. Hydrogels exhibit the ability to swell in water and retain a significant fraction of water within its structure without dissolving. It has physical properties similar to those of human tissues and possesses excellent tissue compatibility. The main disadvantage of hydrogels is their poor mechanical properties after swelling. In order to eliminate the disadvantage, hydrogels can be modified by physical blending or/and chemical modification by grafting, interpenetrating polymer networks and crosslinking method.

The use of hydrogels allows not only delivery of drugs, but also controlled release, in the manner required by the pharmaceutical scientists. For example, drugs can be delivered only when needed, may be directed to specific site, and can be delivered at specific rates required by the body. In the last 20 years, advanced drug delivery formulations have been examined in great detail. Reviews related to the various applications of hydrogels in drug delivery and various sites available in the body for such are readily available. And also we hope to produce materials that are not only intelligent materials but also allow the controlled release of drug of amoxicillin. We also want to investigate drug delivery capability in two pH solutions (pH=1.2 and 7.4 (PBS) that are similar to that of gastric and intestinal fluids.

CHAPTER TWO

MATERIALS AND METHODS

2.1 Materials

Chitosan (highly viscous), poly (ethylene glycol) (M_n=1450) and poly (vinyl alcohol) (M_n=72000) were purchased from Fluka and Sigma–Aldrich, respectively. L(+) tartaric acid was obtained from Carlo Erba. All other chemicals used in this work were analytical grade. Ultrapure water from Milli-Q water system was used to prepare the aqueous solutions. Lysozyme from chicken egg white (50,000 U/mg) was purchased from Sigma-Aldrich and was used without further purification.

2.2 Synthesis of Hydrogel Films

2.2.1 Synthesis of CPT Hydrogel Films

Chitosan (CS) was dissolved in 2% (v/v) acetic acid for overnight to dissolve completely, and then the solution was filtered with cheesecloth to remove undissolved Chitosan. Tartaric acid was dissolved in water and then the pH of solutions adjusts to 6.5 with 0.1M NaOH solution because of using tartarat ions as crosslinker. After the addition of water soluble PEG, the reaction was stirred at 4°C for 30 min in air, and subsequently mixed with the prepared Chitosan solution. Later the reaction mixture was stirred at room temperature for 24h. After that, the mixture was castled on Petri dish was placed in vacuum oven at 60°C for 24 h. Finally, the dried hydrogel films were immersed in 1M NaOH solution for 5h for the removal of residue (unreacted) acetic acid. In the preparation of the hydrogel films, the numbers of moles of NH_2 groups of Chitosan were taken into account. Table 2.1 shows ratio of between CS, PVA and TA.

2.2.2 Synthesis of CVT Hydrogel Films

An amount of Chitosan flake was dissolved in 50 mL of 2% (v/v) acetic acid in a beaker. It was taken one night to dissolve completely and the solution is filtered with

cheese cloth to remove undissolved Chitosan. PVA was dissolved in 10 mL of distilled water (5% w/v) at 70°C for 30 min.

Chitosan solution and PVA solution was mixed to prepare blend solution in a beaker. The blend solution was stirred at room temperature for 30 min. After 30 min, 0.75 g tartaric acid was dissolved in 10 mL of distilled water and then the pH of the solution adjusted to 6.5 with 0.1M NaOH solution. This solution was added to the reaction mixture. The reaction mixture was stirred at room temperature for 90 min. Later, the mixture was castled on Petri dish which was dried at room temperature for 7 days. At the end of the 7 days, the mixture was placed in vacuum oven at 60°C for 24 h. Table 2.1 shows ratio of between CS, PVA and TA.

Table 2.1 Component of CPT and CVT hydrogel films

	Chitosan (g)	PEG (g)	PVA (g)	Tartaric acid (g)	Ratio
CP3T3	1	0.75	-	0.75	4:3:3
CP5 T3	1	1.25	-	0.75	4:5:3
CP10T3	1	2.50	-	0.75	4:10:3
CV3T3	1	-	0.75	0.75	4:3:3
CV5 T3	1	-	1.25	0.75	4:5:3
CV10T3	1	-	2.50	0.75	4:10:3

2.3 Characterization of Hydrogel Films

2.3.1 FTIR Measurements

The Fourier transformed infrared (FTIR) spectra were recorded on the Perkin-Elmer FTIR spectrophotometer Spectrum BX-II to analyze the chemical structure of

CPT and CVT Hydrogel films. Prior to the FTIR measurements, cross linked Chitosan hydrogel film was brought to constant weight in a drying oven at 60ºC for 24 h. The spectra were recorded with the sum of 25 scans at a resolution of 4 cm^{-1} in the range of 4000-400 cm^{-1}. The sample for FTIR measurements was prepared by slicing the film along its thickness direction using microtome.

2.3.2 NMR Analysis

^{13}C and ^{1}H NMR measurements were performed on Bruker DRX-300 and DRX-500 NMR spectrometers by Dr. R. Meusinger in Darmstadt Technical University/ Darmstadt, Germany. Samples (5- 20 mg) were dissolved in 1.5 mL of 20 % (w/w) DCl/D$_2$O at 80°C.

2.3.3 SEM Analysis

The surface morphologies of the samples were studied using a scanning electron microscope at an accelerating voltage of 10 kV. All samples were dried and coated with gold before scanning SEM photographs were taken at different magnifications (in the range of 50–3000x) by using Jeol JSM 60 model SEM apparatus equipped with energy dispersive X-ray (EDX) in Department of Metallurgy and Materials Engineering in Dokuz Eylül University/Izmir, Turkey.

2.3.4 XRD Analysis

The X-ray diffraction (XRD) patterns of the hydrogel films were recorded with oriented mounts, in a Philips X'Pert Pro X-Ray diffractometer using Cu K$_\alpha$ radiation at 45 kV and 40 mA in the 2θ range of 5-60º. These analyses were carried out at the Laboratories of Materials Research Center of İzmir Institute of Technology.

2.3.5 Thermal Analysis

The thermal properties of cross linked Chitosan hydrogel films and Chitosan film were investigated by thermogravimetric analysis (TGA). TGA was performed under nitrogen flow at a flow rate of 10°C/min from 30 to 500°C with a Perkin Elmer Diamond TG/DTA instrument. The weights of the samples varied from 2 to 3 mg.

Thermal properties of the hydrogel films were also characterized by a differential scanning calorimeter (Perkin Elmer Diamond DSC). The dried samples were first heated from 10°C and 300°C under nitrogen atmosphere at a heating rate of 10°C/min and then cooled down to 0˚C then heated again to 300°C.

2.3.6 Enzymatic Degradation

The in vitro degradation of the CPT hydrogel films were followed in 2 mL phosphate buffered solution (PBS, pH=7.4) at 37°C containing 1 mg/mL lysozyme (hen egg white). The samples, after some minutes of degradation, were removed from the medium, dried overnight under vacuum oven at 60°C, and weighed. In order to distinguish enzymatic degradation from the dissolution, the control samples were tested under the same condition as described above, but without adding lysozyme.

2.4 Swelling Measurements

2.4.1 Swelling Test

The swelling behavior of the dried sample films were observed in Phosphate Buffer Solution (PBS) at pH=7.4 and in KCl/HCl Buffer Solution at pH=1.2 at 37°C. After the dried hydrogel films were weighed, they were conditioned at 37°C in the buffer solution at each pH condition. The samples were taken from the medium when they were reached to the equilibrium swelling, wiped with filter paper and weighed. The water content of the film sample was determined according to the following Equation:

$$S\% = \frac{M_s - M_d}{M_s} \times 100 \qquad (2.1)$$

where M_s and M_d represent the weights of swollen and dried state samples, respectively.

2.4.2 pH Sensitivity of Hydrogel Films

Dried hydrogels were left to swell in buffer solution of desired pH (2.6-8.3, I=0.01) at 37°C. Swollen gels then removed from the swelling medium at regular intervals were dried superficially with filter paper, weighed and placed into the same bath. The measurements were continued until a constant weight reached for each sample. The swelling ratios were calculated on a dry basis by using Equation (2.1). In addition, the reversible swelling behavior of hydrogels was also investigated. The samples that reached equilibrium at pH=2.6 were allowed to reach pH=8.3 and then back to pH=2.6 medium again.

2.4.3 Thermal Sensitivity of Hydrogel Films

In order to determine the temperature sensitivity of hydrogels, dynamic swelling measurements were performed by gravimetric means at 4 and 37 °C. The samples were dried to the constant weight in vacuum and then immersed in a constant temperature bath filled with PBS (pH=7.4, I=0.2). The samples were removed from the PBS at appropriate intervals, blotted with filter paper, weighed and then returned to PBS. This procedure was repeated until the equilibrium was reached. The swelling ratios were calculated on a dry basis by using Equation (2.1). All swelling experiments were repeated in an incubator (GLF 1086) at least three times and the results reported as averages.

2.5.2 Release Study

Drug loaded samples (25 mg amoxicillin g^{-1} hydrogel) were also prepared using a similar method for release experiments. The in vitro release of the entrapped drug, amoxicillin, were carried out by placing the hydrogel film samples loaded with the drug into 10 mL of solution with pH=1.2 and 7.4 at 37 ºC in water bath. At periodic intervals 0.5 mL of solution containing drug were withdrawn and tested at λ_{max}=395 nm using Shimadzu 160A model UV-VIS spectrophotometer. The amount of released amoxicillin was calculated using appropriate calibration curve. The same release experiments were also carried out for solution with pH=7.4 (in PBS) at 37º.

CHAPTER THREE

RESULTS AND DISCUSSION

3.1 Characterization of The Prepared Hydrogel Films

3.1.1 Fourier Transform Infrared (FTIR) Spectra of the Samples

3.1.1.1Fourier Transform Infrared (FTIR) Spectra of the CPT Hydrogel Films

The structure of CPT Hydrogels was analyzed by using FTIR spectroscopy. Figure 3.1 shows FTIR spectra of Chitosan and its hydrogels.
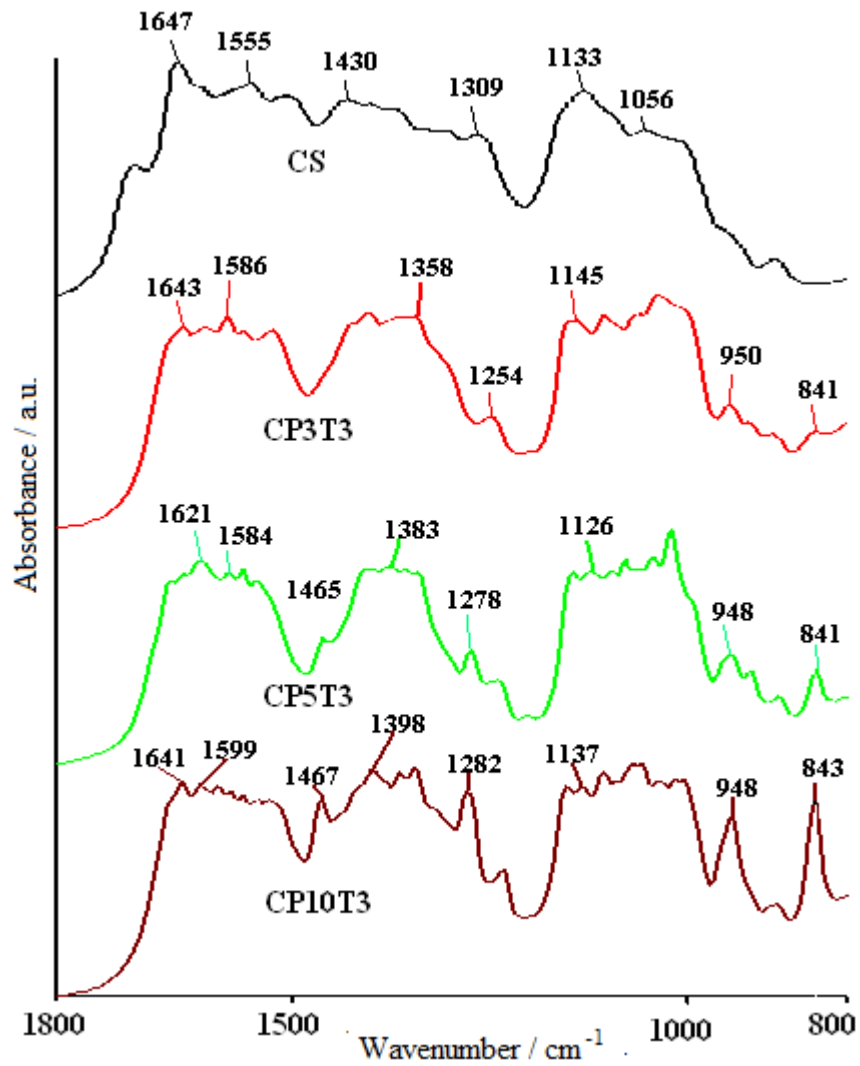

Figure 3.1 FTIR spectra of Chitosan film and CPT hydrogel films

The spectrum of Chitosan film exhibits absorption bands around 1647 and 1555 cm^{-1} which represent the amide I (C=O stretching) and amid II (N-H deformation) bands, respectively (Cao et al., 2005 and Tanuma et al., 2010). Chitosan has characteristic C–H bending bands at 1309 cm^{-1} and 1430 cm^{-1}. The absorption bands at 1133 cm^{-1} (asymmetric stretching of C–O–C bridge), 1056 cm^{-1} (C–O stretching) were characteristics of its saccharine structure (Kurita et al.,2001, Qu et al., 2000, and Kolhe et al., 2003). Pure PEG has characteristic bands at 1280, 947, and 843 cm^{-1} (Bhattarai et al., 2005). While FTIR spectrum of CPT Hydrogel films were compared with chitosan film spectrum, intensity of the amide I band at 1647 cm^{-1} and the amide II band significantly decreased. This resultant spectrum showed that the –NH$_2$ groups of Chitosan were partially interacted with PEG. The characteristic bands associated with PEG in CPT at 1280, 948, and 841 cm^{-1} were significantly increased with the increasing amounts of PEG. The bands at 1120 and 2880 cm^{-1} in CPTs were attributable to the superposition of C–O and C–H stretching vibrations of Chitosan and PEG. In addition, the formation of the cross-linked structure was confirmed by the absorption band at 1380 cm^{-1} (Figure 3.1). The intensity at 1380 cm^{-1} increased with the content of PEG of the CPT hydrogel films. This 1380 cm^{-1} absorption band caused by the PEG CH$_2$ deformation vibration, since the number of the CH$_2$ groups was increased with preceding the cross-linked reaction.

3.1.1.2 Fourier Transform Infrared (FTIR) Spectra of the CVT Hydrogel Films

FTIR spectroscopy was used to assess the polymer chemical groups (Chitosan and PVA) and investigating the formation of crosslinked networks from the CVT Hydrogel films with tartaric acid and PVA. Figure 3.2 shows the FTIR spectra relative to the Chitosan, Chitosan film (CS) and CVT Hydrogel films. In Figure 3.2 spectrum of pure Chitosan shows bands around 893 and 1156 cm^{-1} corresponding to saccharide structure (Shigemasa, Matsuura, Sashiwa, & Saimoto, 1996). In spite of the several bands clustering in the amide II band range from 1510 to 1570 cm^{-1}, there were still strong absorption bands at 1637 and 1547 cm^{-1}, which are characteristic of Chitosan and have been reported as amide I and II bands, respectively.
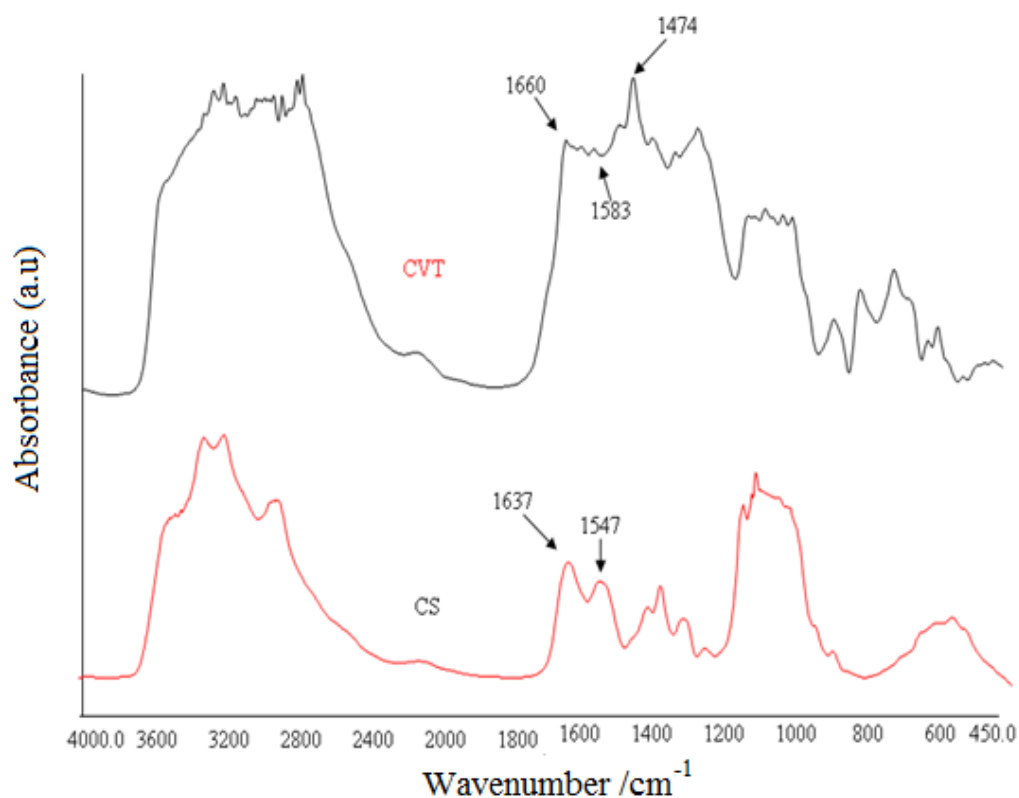
Figure 3.2 FTIR Spectra of Chitosan and CVT hydrogel

The sharp bands at 1383 and 1424 cm^{-1} were assigned to the CH$_3$ symmetrical deformation mode. The broad bond at 1030 and 1080 cm^{-1} indicates the C-O stretching vibration in Chitosan. Another broad band at 3433 cm^{-1} is caused by amine N-H symmetrical vibration, which is used with 1637 cm^{-1} for quantitative analysis of deacetylation of Chitosan. Bonds at 2866 and 2900 cm^{-1} are the typical C-H stretch vibrations (Brugnerotto et al., 2001; Costa & Mansur, 2007, 2008; Rao, Naidu, Subha, Sairam, & Aminabhavi, 2006; Shigemasa et al., 1996; Wang et al., 2004a, 2004b). The FTIR spectra of the CVT hydrogel film presented in Figure 3.2 is different from that of the Chitosan because of the ionization of the primary amino groups. There are two distinct bonds at 1474 and 1583–1660 cm^{-1}. Formation of the 1583–1660 cm^{-1} bond is the symmetric deformation of –NH$^{+}_3$ resulting from ionization of primary amino groups in the acidic medium whereas the bond at 1474 cm^{-1} indicates the presence of carboxylic acid in the polymers. Due to the amid II band at 1660 cm^{-1}, the characteristic band of carboxylic acid was not appeared. The bond at 1210–1300 cm^{-1} is due to the C-H vibration. Hence, there is a significant

reduction of intensities from the main absorption bands related to Chitosan, for instance amine region (1583–1660 cm^{-1}).

The FTIR spectrum of pure PVA is reported by Ezequiel et al. 2009, where all major bands related to hydroxyl and acetate groups were observed. More specifically, the broad band observed between 3550 and 3200 cm^{-1} is associated with the stretching O-H from the intermolecular and intramolecular hydrogen bonds. The vibrational band observed between 2840 and 3000 cm^{-1}refers to the stretching C-H from alkyl groups and the bonds between 1750 and 1735 cm^{-1} are due to the stretching C=O and C-O from acetate group remaining from PVA (Mansur & Costa, 2008; Mansur, Sadahira, Souza, & Mansur, 2008; Suh & Matthew, 2000).

It can be noted that the bands at 1110, 1430, 1637 and 1660 cm^{-1} mainly associated with PVA, and also the presence of bands related to carboxylic acid and the imines formed by the crosslinking reaction by tartaric acid of amine groups from Chitosan. Moreover, an increase in the intensity and a shift in the band associated with the bend vibration of the CH$_2$ (1430 cm^{-1}) group was observed. Chemical crosslinking of the Chitosan/PVA blends can be explained by the Schiff base formation as verified by the 1638 and 1538 cm^{-1} bands associated with the C=N and NH$_2$ groups, respectively (Costa & Mansur, 2008; Rokhade, Patil, & Aminabhavi, 2007; Wang et al., 2004a, 2004b). All Chitosan-derived blends have shown a relative increase on their imine (-C=N-) band (1660 cm^{-1}) and simultaneous drop on the amine (-NH$_2$) band after chemical crosslinking with tartaric acid. The imine group was formed by the nucleophilic reaction of the amine from Chitosan.

3.1.2 NMR Spectroscopy

3.1.2.1 NMR Analysis of CPT Hydrogel Film

NMR spectrum of CPT was shown in Figure 3.3. Typical peaks at 3.4 ppm and 3.6 ppm were assigned to the ring methyne and methylene protons of Chitosan saccharide units and methylene groups of PEG (Xing et al., 2010 and Sugimoto et al., 1998). Peaks at 3.8 ppm and 2.1 ppm attributed to –CHNH$_2$ and –COCH$_3$, but these peaks were not observed at [1] H NMR spectrum. Methylene protons and –OCH$_2$ peaks from PEG were appeared at 1.6 ppm and 3.4 ppm, respectively.

Furthermore, the analysis of CPT ^{13}C NMR spectrum showed the peak at 71 ppm attributed to $-CH_2-$ groups of the $-O-CH_2-CH_2-O-$ chain (Sugimoto et al., 1998). Also the peaks at 173 ppm and 184 ppm referred to $-NH-CO-$ and $C=O$ groups of tartaric acid.
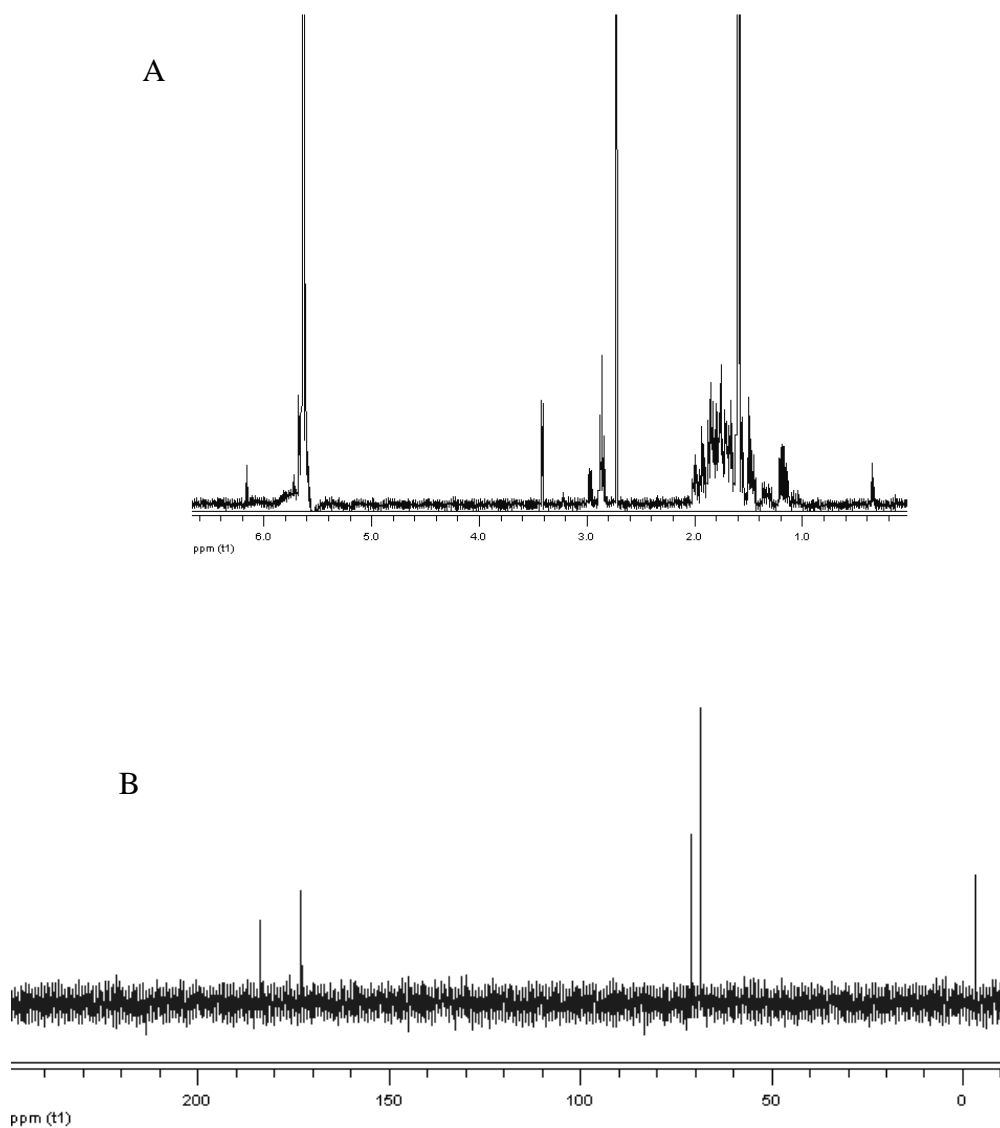

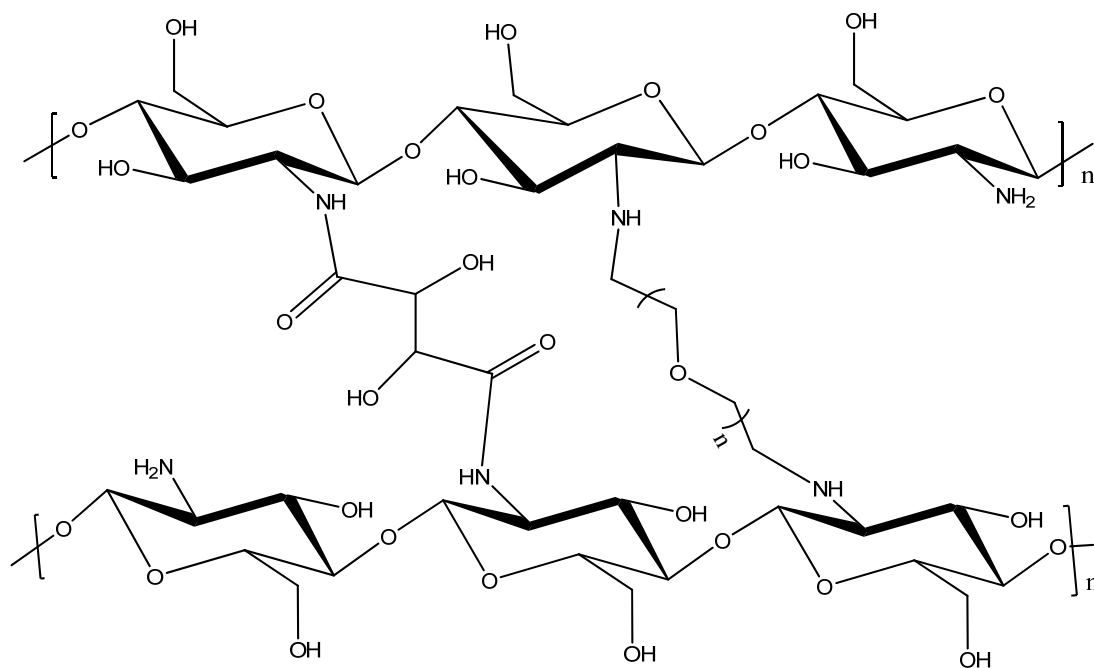Figure 3.3 ^{1}H NMR spectrum of CPT (A), ^{13}C NMR spectrum of CPT (B) both at 70°C.

Figure 3.4 Proposal of the crosslinked structure

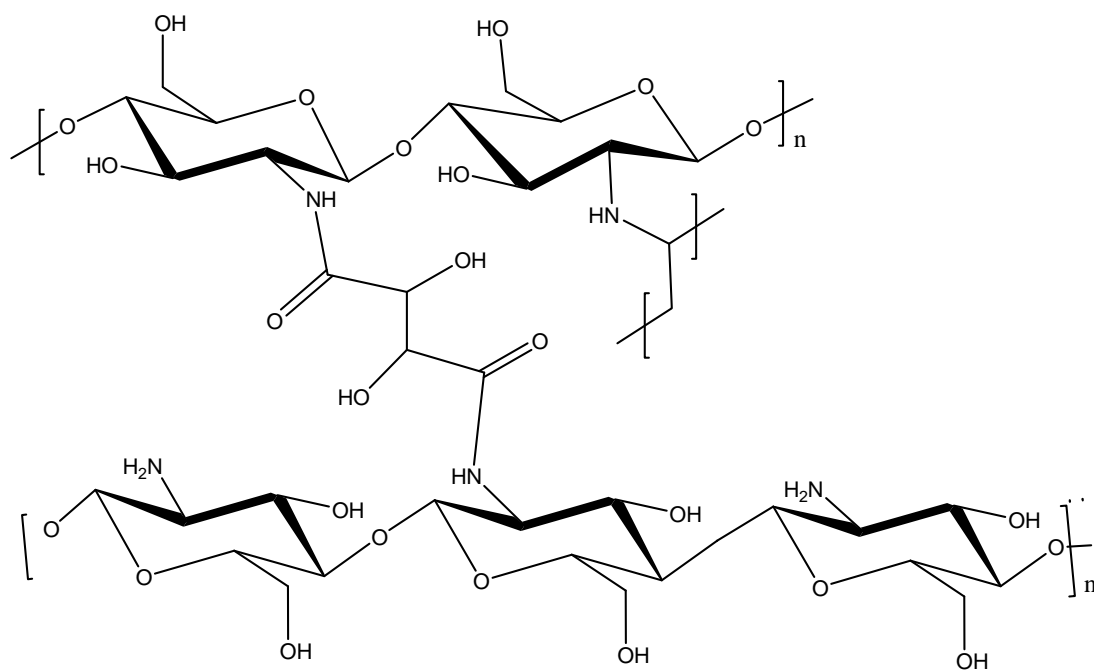## 3.1.2.2 NMR Analysis of CVT Hydrogel Film

Figure 3.5 Proposal of the crosslinked structure

The NMR spectrum of CVT is shown in Figure 3.6. The peaks of the vinyl groups at 5.8 and 6.3 ppm PVA (Yong, Sung, & Sohk, 2000) do not appear in CVT spectrum. Disappearances of these peaks showed the interaction between amino groups of Chitosan and vinyl groups of PVA. Also, the new peaks at 2 ppm and 2.8 ppm which were indicated that crosslinked with TA and PVA in ^{1}H NMR spectrum in Figure 3.6 A. Looking at [13] C NMR, the new peaks at 40 ppm, 70 ppm and 170 ppm which were shown that crosslinking with PVA and TA.
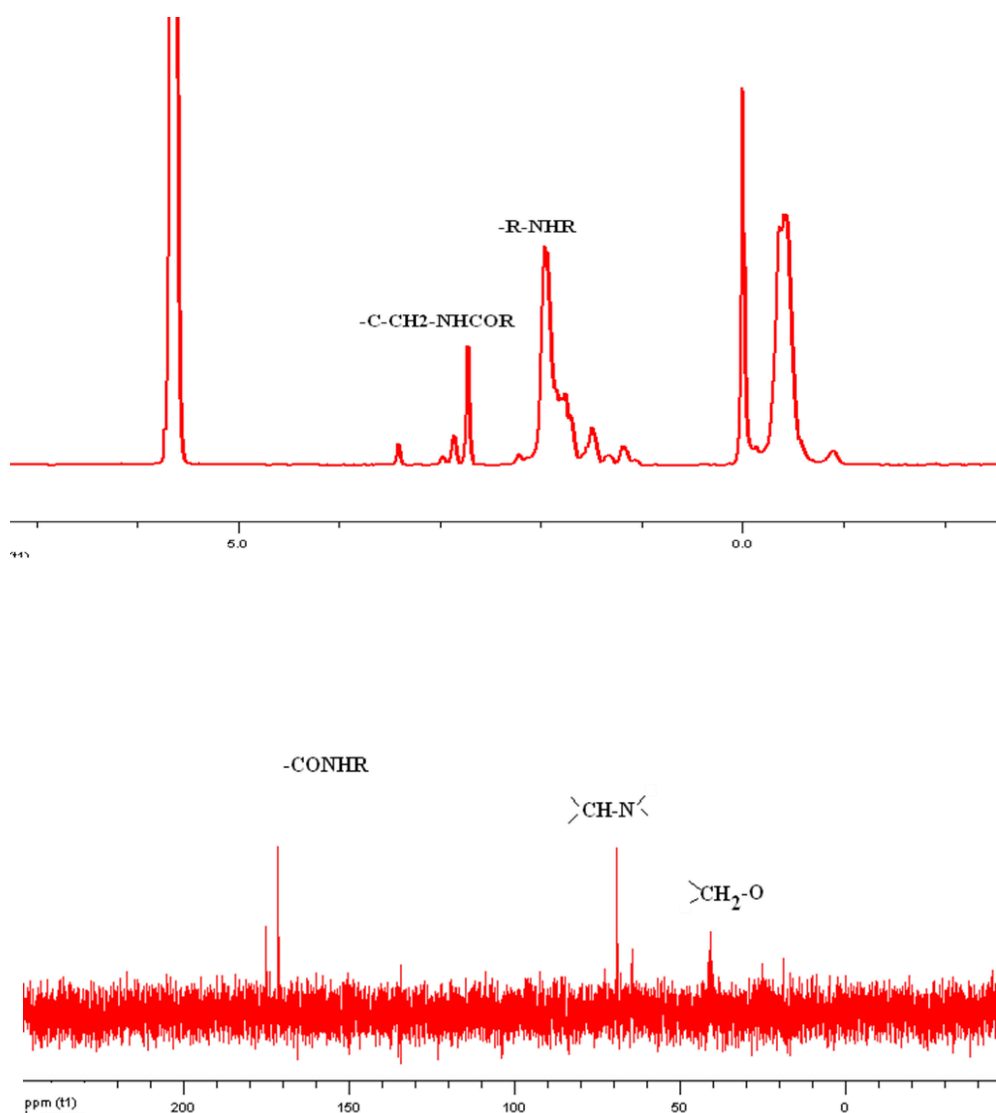

Figure 3.6 ^{1}H NMR spectrum of CVT (A), ^{13}C NMR spectrum of CVT (B)

After the evaluation of the FTIR data and NMR spectra, the proposal of the structural formula of the synthesized hydrogels were given in 3.4 and 3.5.

3.1.3 SEM Analysis

3.1.3.1 SEM Analysis of CPT Hydrogel Films

The surface morphology of CPT and CS hydrogels were investigated with SEM analysis in Figure 3.7. As shown in Figure 3.7 a, Chitosan hydrogel have spherical surface morphology, on the other hand this spherical morphology does not appear in SEM image of CPT hydrogel.

At the same time, the small holes on the surface were disrupted and different structures such as fibrous morphology have begun to create.

As shown in Figure 3.7c and 3.7d, by the increase in the amounts of PEG caused fibrous structure. In addition, these fibrous structures may be an indication of the interaction between PEG and CS.
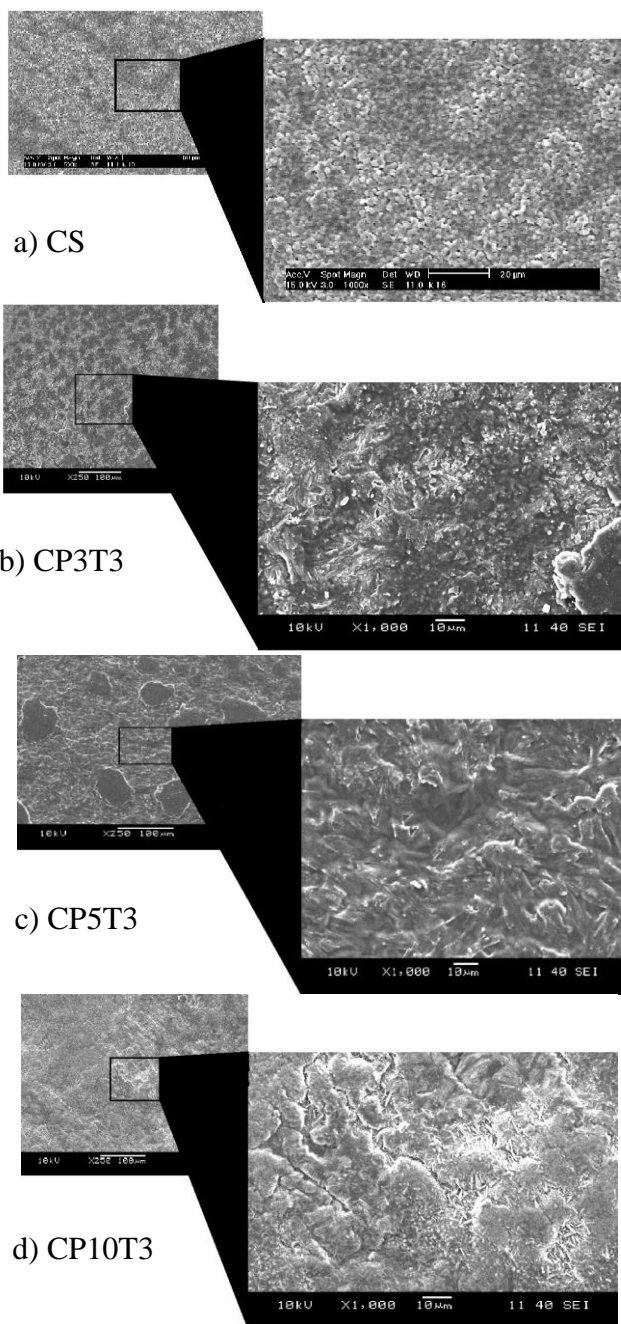
a) CS

b) CP3T3

c) CP5T3

d) CP10T3

Figure 3.7 The SEM images of Chitosan and the CPT Hydrogels
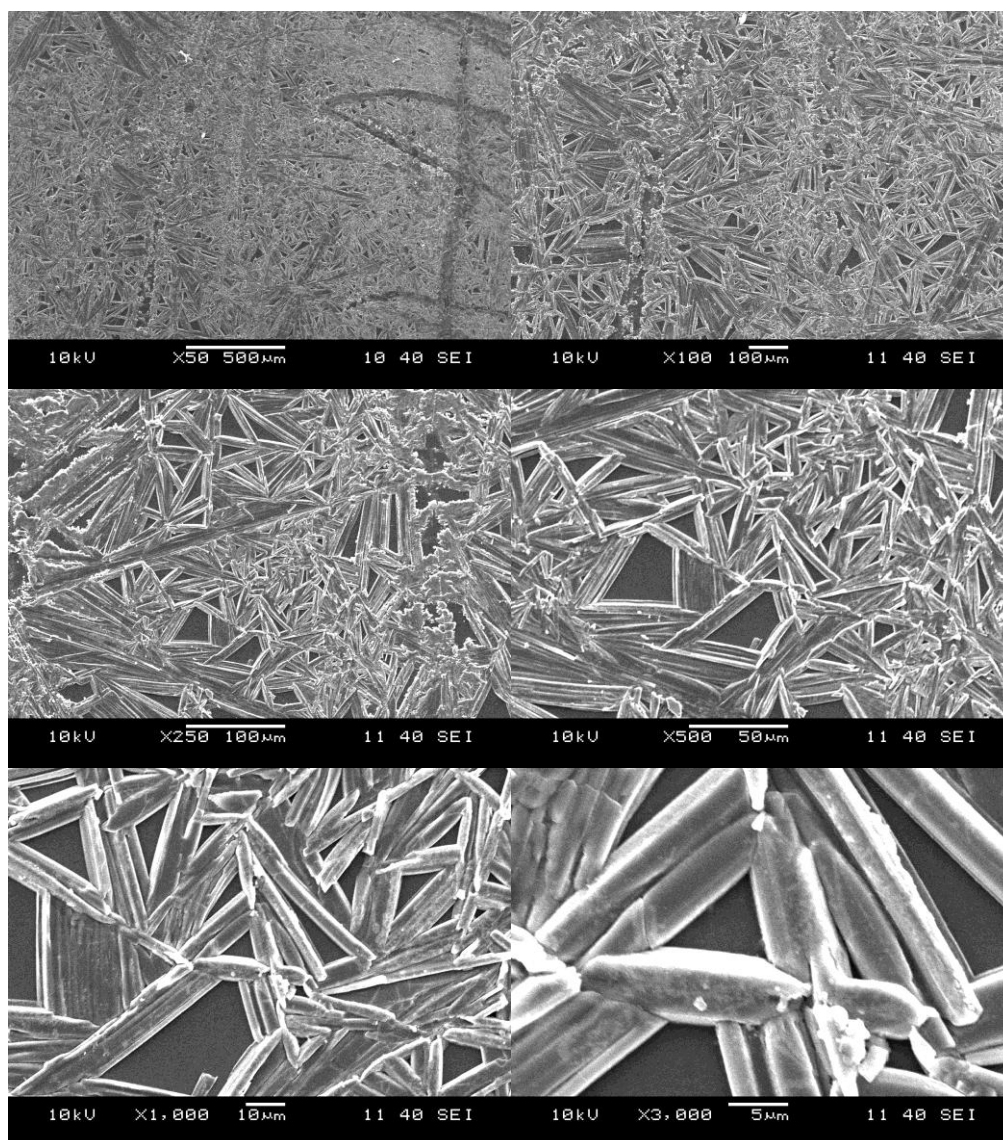
3.1.3.2 SEM Analysis of CVT Hydrogel Films

Figure 3.8 The SEM images of CVT hydrogel

Figure 3.8 shows the SEM images of CVT hydrogel films. SEM images indicate that CVT surface morpholgy was changed as CS. There are very small sphere in CS film surface in Figure 3.8 but after crosslinking reaction, spheres had become thinner fibers, as shown in Figure 3.8. In addition, these fibrous structures may be an indication of the interaction between PVA and CS. On the other hand crystal structure of CVT hydrogel increased with crosslinking as CS hydrogel. This result was supported by XRD analysis results given in the next section.

3.1.4 XRD Analysis

3.1.4.1 XRD Analysis of CPT Hydrogel Films

The crystallographic structure of Chitosan and CPT hydrogel films were determined by XRD. As presented in Figure 3.9, the XRD pattern of a Chitosan sample shows a characteristic peak at $2\theta=20°$ caused by the presence of (001) and (002), we agreed with the results given in Wang & Hon, 2005. As well known, Chitosan with high deacetylation degree could not be soluble in water due to its strong intermolecular hydrogen bond. In generally, for the Chitosan diblock copolymer, the peak associated with Chitosan at about 20° decreased. This result indicated that crystalline structure has been disrupted to a great extent by the chemical bond between Chitosan and other polymer structure in the diblock copolymer (Kong et al., 2010). The intermolecular hydrogen bonds in Chitosan diblock copolymer have decreased obviously in comparison with that of Chitosan, and as a result, the water solubility of the material was significantly improved (Zhu, Chen, Yuan, Wu, & Lu, 2006).

However, in this study, the intensity of the characteristic peak of Chitosan at 20° was increased with increasing amount of PEG. Also, the new peaks were formed at $2\theta=10°$ and 15°. The intensity of this peak was increased from CP3T3 to CP10T3, because of the increasing PEG amounts.

In particular, as the molar ratio of Chitosan to the CPT hydrogel decreasing from CP3T3 to CP10T3, this is due to the high content of PEG promoting the crystal growth of the CPT hydrogels (Teng et al., 2010).
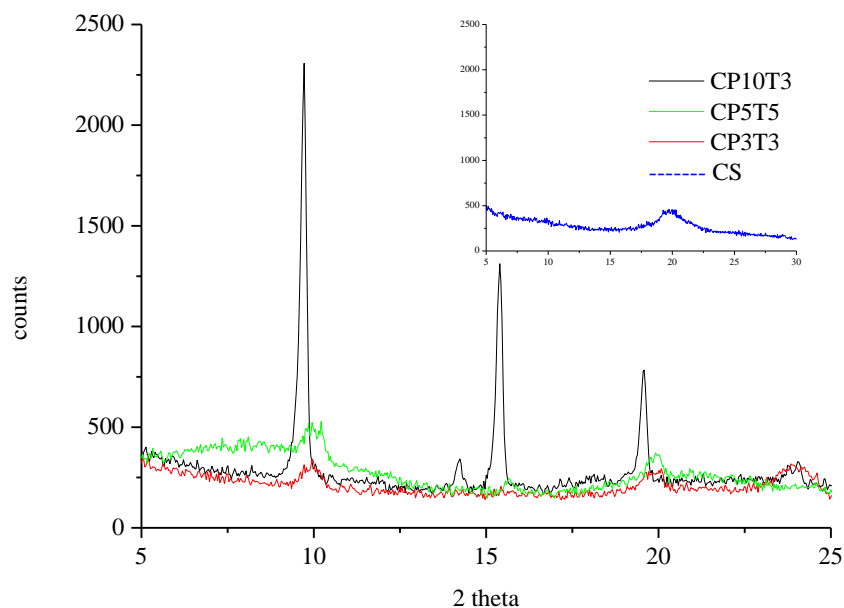
Figure 3.9 X- Ray diffraction patterns for Chitosan and CPT hydrogel films.

3.1.4.2 XRD Analysis of CVT Hydrogel Films

The X-ray diffraction patterns of Chitosan and CVT hydrogel film were shown in Figure 3.10. X-ray diffraction (XRD) analysis was applied to characterize the crystallinity of native and cross linked Chitosan. Generally, the XRD patterns of all types of Chitosan show crystalline peak approximately at $2\theta=20°$ (Qin, et al., 2003).

The results show that Chitosan and crosslinked Chitosan yield similar XRD patterns, with a characteristic peak at $2\theta= 20.3°$. However, the cross linked Chitosan with longer length of cross linking agents show higher and sharper crystalline peaks as compare to those with non-crosslinked Chitosan. Thus it appears that when Chitosan is crosslinked with PVA and TA there is a change in the crystalline structure. The crystallinty of Chitosan hydrogel film increased with crosslinking reaction in CVT hydrogel film. As a consequence, there seem to be an obvious correlation between the crosslinking and the rise in crystallinity due to recrystallization of CVT hydrogel film.
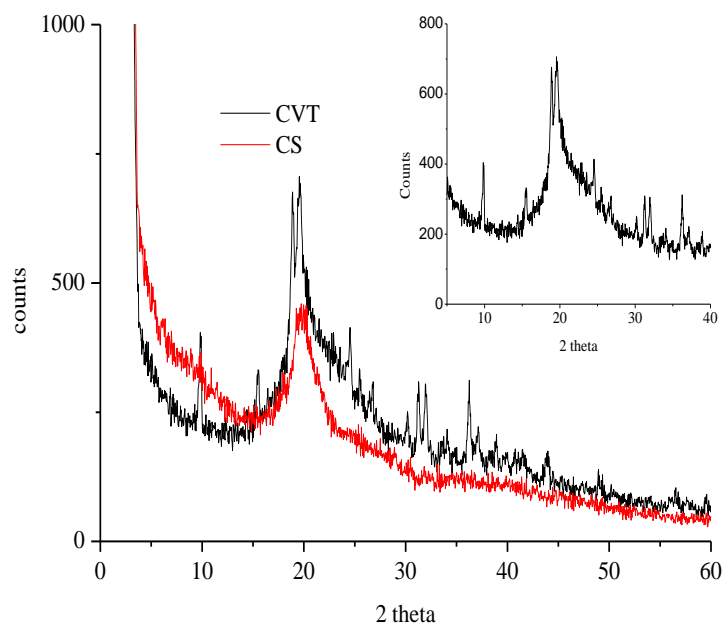
Figure 3.10 X-Ray diffraction patterns of Chitosan and CVT Hydrogels films.

On the other hand, crystal structures of two polymorphs of Chitosan, tendon (hydrated) and annealed (anhydrous) polymorphs, have been reported (Ogawa, Yui, & Okuyama; 2004). In as much as Chitosan is a polymer of d-glucosamine that has free amino group, it is a cation polymer making salt with an acid. Crystal structures of several Chitosan salts with inorganic and organic acids have been studied Ogawa et al., 2004.

The characteristic peaks of type II at $2\theta = 22°$, $19.8°$ and $10.2°$. Based on all this information, we might say that CVT hydrogel film mainly show the tendon (hydrated) polymorphs crystal structure.

3.1.5 Thermal Analysis

3.1.5.1 Thermal Analysis of CPT Hydrogel Films

Differential scanning calorimeter (DSC) and thermogravimetric analysis (TGA) were selected to characterize the thermal properties of CPT film. Thermal decomposition behaviors of CPT films and Chitosan films were performed by TG/DTG analysis and DSC analysis in Figure 3.11 and 3.12, respectively. There

were three degradation stages in the thermograms. The first stage showed decomposition of water at 56°C, 119°C, 122°C, and 76°C for Chitosan, CP3T3, CP5T3 and CP10T3, respectively. The temperature of degradation (T_d) of Chitosan film was 250°C. In the thermograms, CPT films have two stages of mass losses which were due to the degradation of the samples. The first stage mass loss was observed at the temperature range of 257-286°C with a total of 33-18% mass loss. On the other hand, the samples were then completely degraded at 402-473°C which might be attributed to the PEG and TA in Chitosan. The results were summarized in table 3.1.
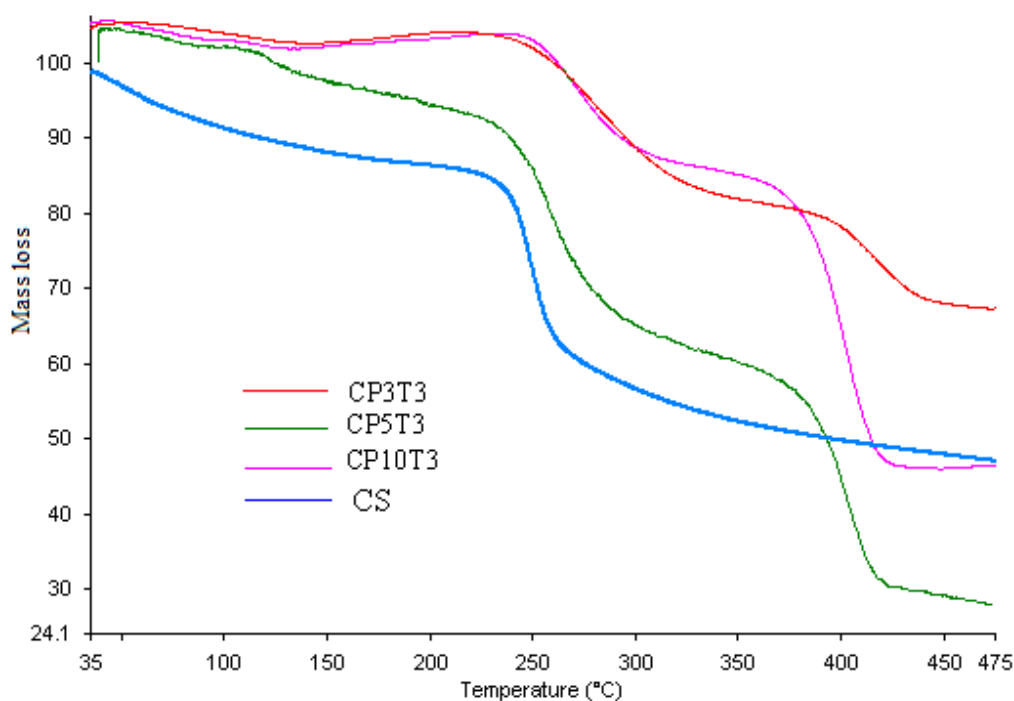

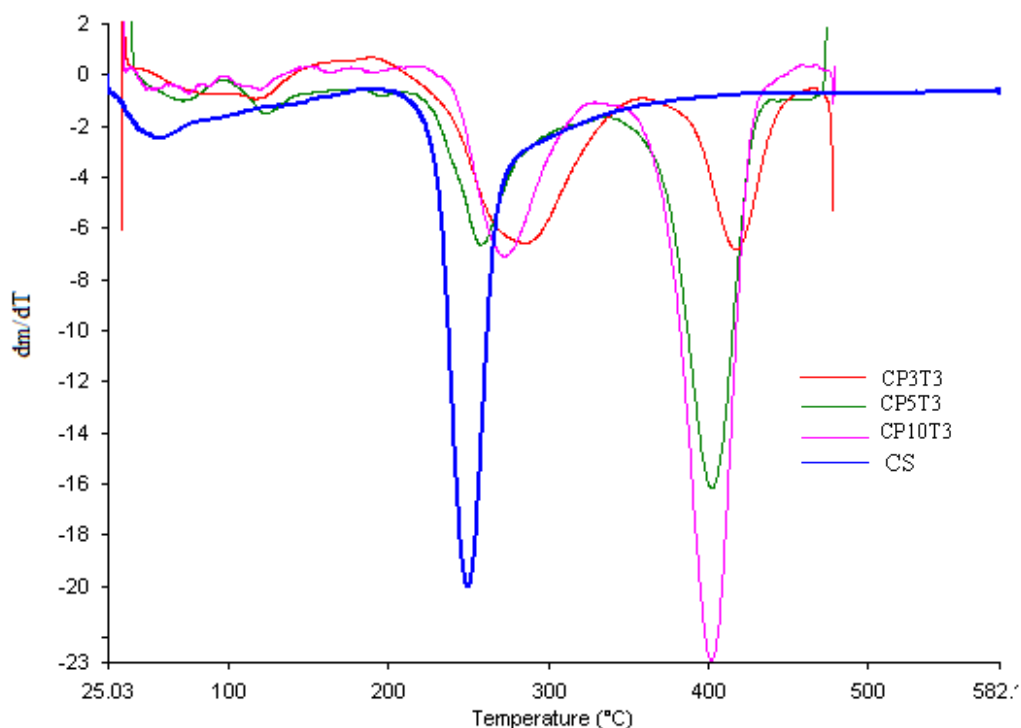Figure 3.11 Thermogravimetric curves of Chitosan and its hydrogels.

Figure 3.12 DTG curves of Chitosan and CPT hydrogel films.

Table 3.1 Results of thermogravimetric analysis in nitrogen flow

Sample	First stage		Second stage		Third stage	
	T(°C)	Mass loss %	T(°C)	Mass loss %	T (°C)	Mass loss %
Chitosan	25-105	13	230-270	38	-	-
CP3T3	53-146	6	235-332	22	432-477	14
CP5T3	68-144	10	235- 285	33	370-402	33
CP10T3	75-83	2	243-310	18	372-477	40

It has been observed in the DSC profiles of Chitosan that did not melt or degraded between 20 and 200°C as shown (Xing, Xiang, Shuai, Ying, Li, Gang, Feng, Xia, Yu, Zhi, 2010). However, in this study, a broad endothermic peak centered at the temperatures between 40 and 130°C were observed for the DSC curves of the Chitosan film and CP3T3 samples in Figure 3.13. This peak was caused by the overall endothermic process connected with the evaporation of bound water. In general, polysaccharides have a strong affinity for water and can be easily hydrated

in the solid state (Tanuma, 2009). For this reason, the broad peak was also observed for the hydrogel films. Whereas, CPT film samples also showed a sharp endothermic peak centered at the temperatures between 40 and 50°C. This may be attributed to the melting of the PEG moiety. The intensity of this endothermic peak of the CPT hydrogel films was increased with the increase in the amounts of PEG. The endothermic enthalpy (ΔH) values were calculated from the area under the endothermic peak caused by the melting of the CPT Hydrogels. The melting enthalpies of these samples were determined by DSC measurements were different in some respect from that of the PEG/ Chitosan blend samples. TG/DTG and DSC analysis results were summarized in Table 3.2.
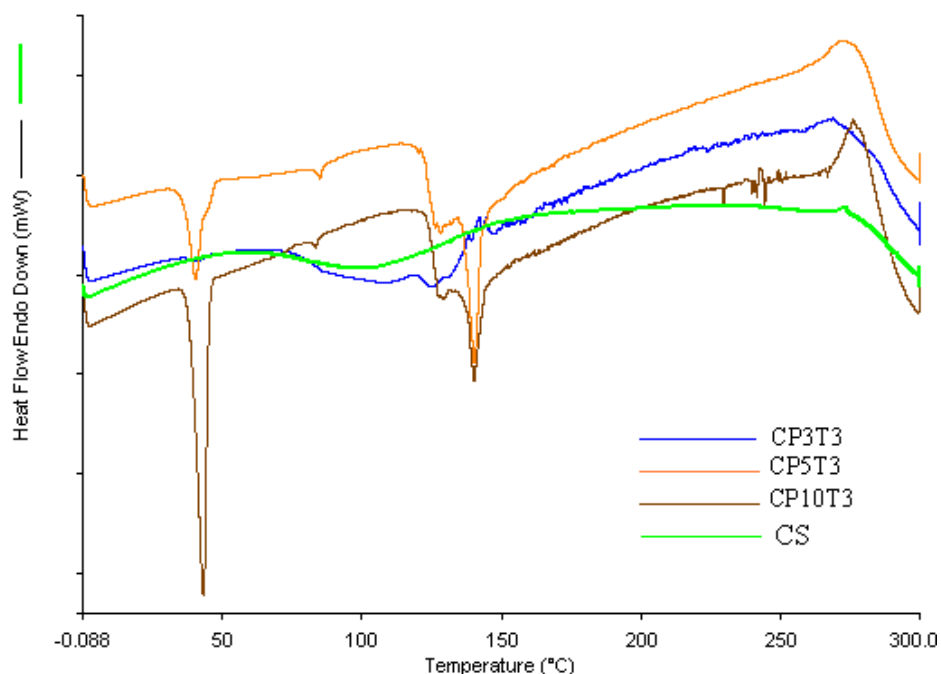

Figure 3.11 The DSC heating curves of Chitosan and CPT Hydrogels

Table 3.2 Melting point, Enthalpy of fusion and Decomposition temperature of CPT Hydrogels

	Melting point (°C)	Enthalpy of Fusion (J/g)	Decomposition temperature (°C)
CP3T3	40.0	1.3	271
CP5T3	40.4	27.3	274
CP10T3	43.0	58.7	279

3.1.5.2 Thermal Analysis of CVT Hydrogel Films

Differential scanning calorimeter (DSC) and thermogravimetric analysis (TGA) were selected to characterize the thermal properties of CVT film. Thermal decomposition behaviors of CVT and Chitosan films were performed by TG/DTG analysis. As indicated in Figure 3.14, there were three degradation stages in the thermograms. The first stage showed decomposition of water at 55°C and 34°C, for Chitosan and CVT respectively. The temperature of degradation (T_d) of Chitosan film was 249°C. In the thermograms, CVT films have two stages of mass losses which were due to the degradation of the samples. The first stage mass loss was observed at the temperature range of 257 °C and second stage was completely degraded at 402-473°C which might be attributed to the PVA and TA onto hydrogel.
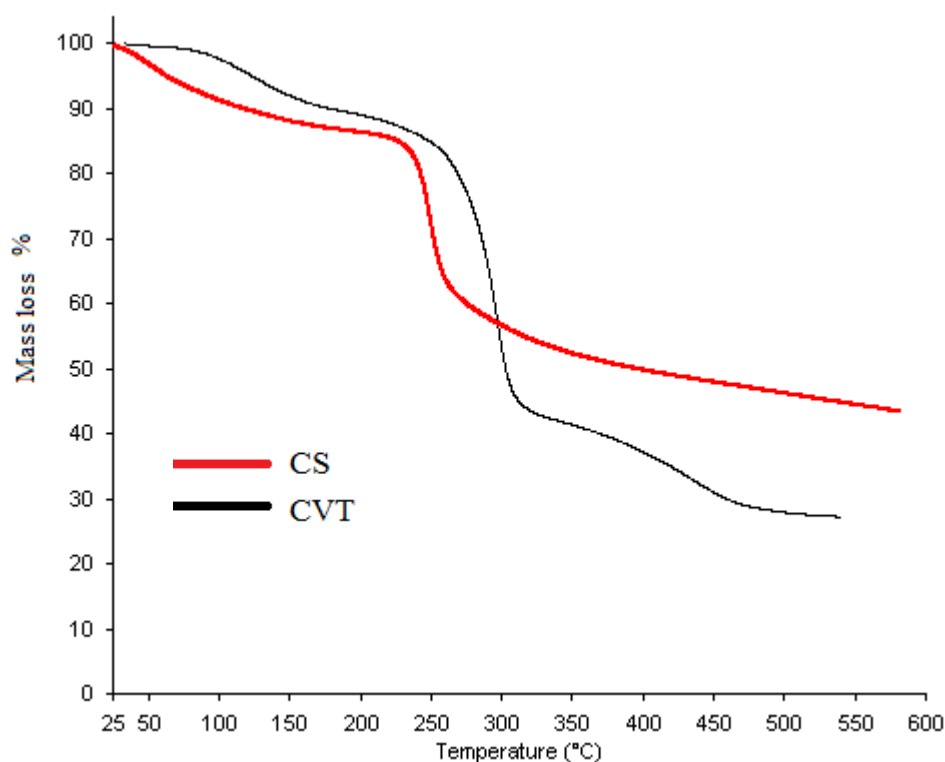

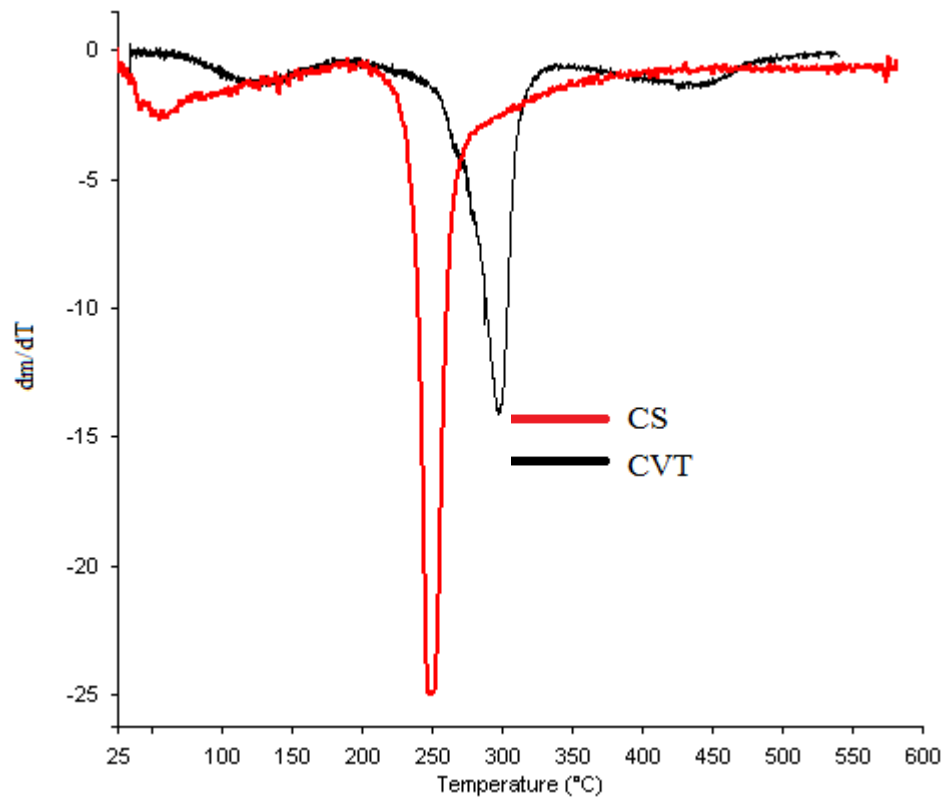Figure 3.14 Thermogravimetric curves of Chitosan and CVT hydrogel in nitrogen flow

Figure 3.15 DTG curves of Chitosan and CVT hydrogel in nitrogen flow
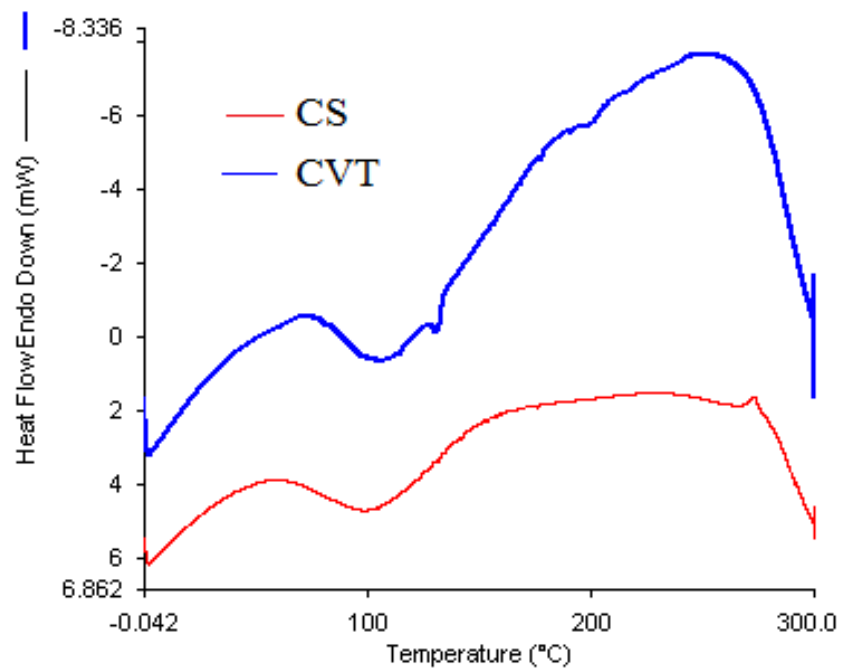

Figure 3.16 the DSC heating curves of Chitosan and CVT hydrogel

Table 3.3 Results of thermogravimetric analysis in nitrogen flow

Sample	First stage		Second stage		Third stage	
	T(°C)	Mass loss %	T(°C)	Mass loss %	T (°C)	Mass loss %
Chitosan	55	13	249	43	-	-
CVT	34	11	297	47	426	15

Table 3.4 Melting point, Enthalpy of Fusion and Decomposition temperature of CPT

	Melting point T (°C)	Enthalpy of Fusion (J/g)	Decomposition temperature (°C)
CS	76	22.5	211
CVT	90	25.9	259

It has been observed in the DSC profiles of Chitosan that it did not melt or degraded between 20 and 200°C as shown in literature (Xing et. al., 2010). However, in this study, a broad endothermic peak centered at the temperatures between 80 and 110°C were observed for the DSC curves of the Chitosan film and CVT samples. This may be attributed to the melting of the CVT hydrogel films. Enthalpy of fusion (ΔH) values were calculated from the area under the endothermic peak caused by the melting of the CVT Hydrogels. TG/DTG and DSC analysis results were summarized in Table 3.3 and 3.4 for CVT hydrogel.

3.1.6 Enzymatic Degradation

3.1.6.1 Enzymatic Degradation of CPT Hydrogel Films

In human body, Chitosan is mainly degraded by lysozyme. The in vitro degradation behavior of Chitosan has been usually investigated by using hen egg white (HEW) lysozyme (Etienne et al., 2005 , Freier et al., 2005 and Neamnark et al., 2007, because HEW lysozyme as well as human lysozyme cleavages the b(1-4)-linked GlcNAc and GlcN subunits of Chitosan (Nordtveit, Varum, & Smidsrod, 1996)
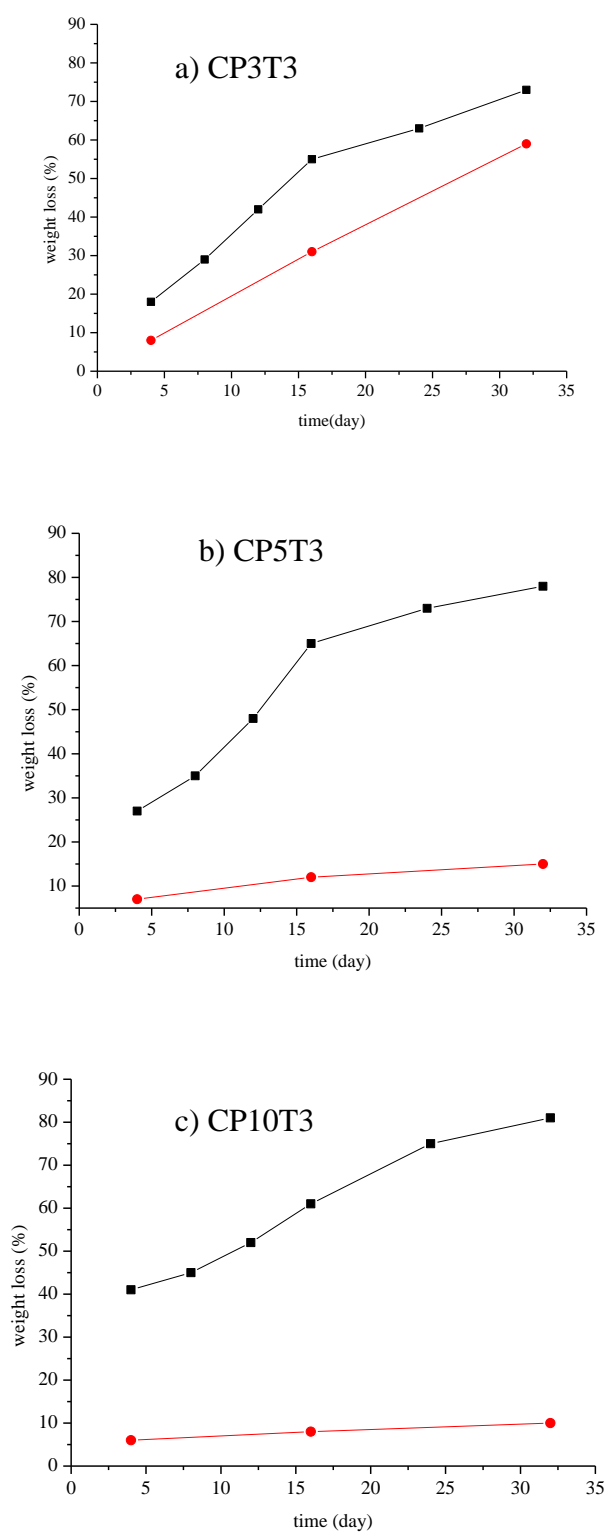
Figure 3.15 Weight losses of hydrogel films in 1 mg /mL lysozyme / PBS and in PBS without lysozyme at 37 °C as a function of time. Black and red mark shows the sample of with and without lysozyme, respectively.

In this study, the degradation behavior of the hydrogel film in the presence and in the absence of lysozyme was investigated in PBS at 37°C (Figure 3.17). Figure 3.17a showed the degradation behavior of the CP3T3 film sample. The mass loss of CP3T3 at most 59 even after 32 days in PBS without lysozyme, while in the presence of 1 mg/mL lysozyme, the mass loss reached to more than 73 % after 32 days. Similarly, the mass loss of CP5T3 at most 15% even after 32 days in PBS without lysozyme, while in the presence of 1 mg/mL lysozyme, the mass loss was more than 78% after 32 days and it was proportional to the degradation time. The degradation behavior of CP10T3 was shown in Figure 3.17c. The mass loss of CP10T3 degraded with 1 mg/mL lysozyme was more than 81 % after 32 days.

From these results, the tendency of the enzymatic degradation rates the samples was found to be paralleled with that of the swelling ratio at the next section. On the other hand, this tendency was not the same as far as the samples with different ratio of PEG. This was due to the fact that the CP10T3 has more dispersed cross-linked point and lysozyme may easily access the binding site of Chitosan molecular chain. Thus, the swelling ratio and the internal structure were influenced the enzymatic degradation.

3.1.6.2 Enzymatic Degradation of CVT Hydrogel Films

It is well known that, in human serum, N-acetylated Chitosan is mainly depolymerized enzymatically by lysozyme, and not by other enzymes or other depolymerization mechanisms (Varum, Myhr, Hjerde, and Smidsrod, 1997). The enzyme biodegrades the polysaccharide by hydrolyzing the glycosidic bonds present in the chemical structure. Lysozyme contains a hexameric binding site (Pangburn, Trescony, Heller, 1982). and hexasaccharide sequences containing 3–4 or more acetylated units contribute mainly to the initial degradation rate of Nacetylated Chitosan (Nordtveit, Varum, Smidsrod, 1994).

As shown in Figure 3.18, enzyme breaks down the structure by attacking the 1-4 bond of the beta. PVA and TA connected with amino groups of Chitosan while increasing of steric effect and to prevent the passage of the enzyme attacked. As seen

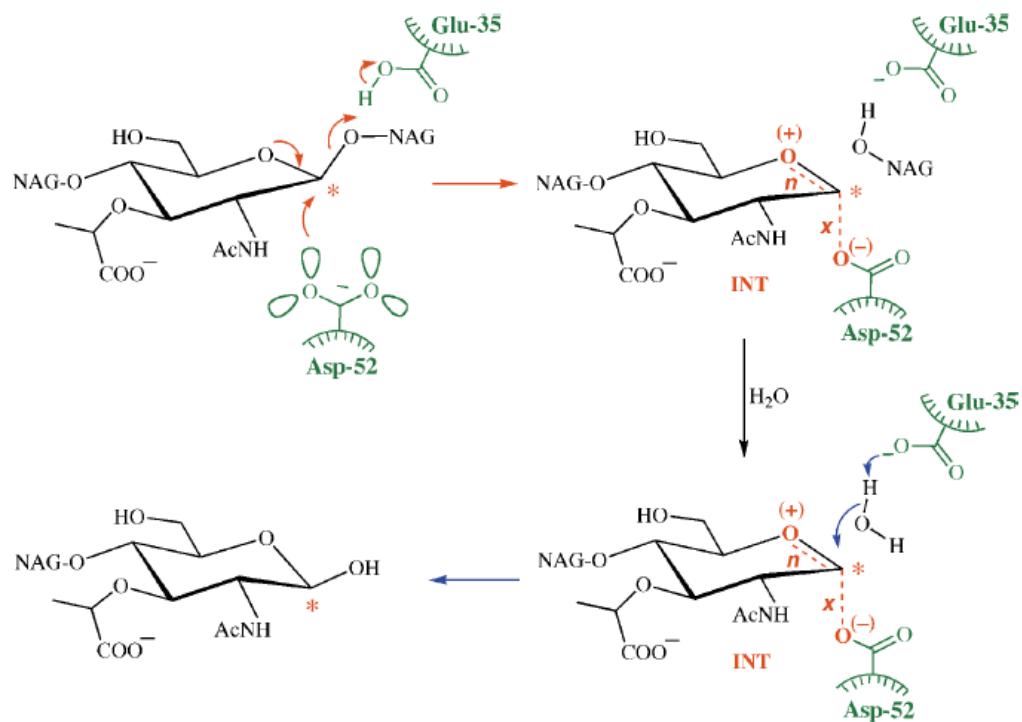in Figure 3.19 cross-linked CVT films were broken down more slowly according to the pure Chitosan film.

Figure 3.18 The reaction catalyzed by lysozyme. The substrate is bound so that the leaving group oxygen, the 4-OH group of an N-acetylglucosamine (NAG) residue, is protonated as it leaves by the COOH group of Glu 35. Groups on the enzyme are colored green, electron movements and the key developing bonds and charges in red. Only one of the dashed *exo* and *endo* (*x* and *n*) bonds of the intermediate (INT) is actually present: which one defines the mechanism.
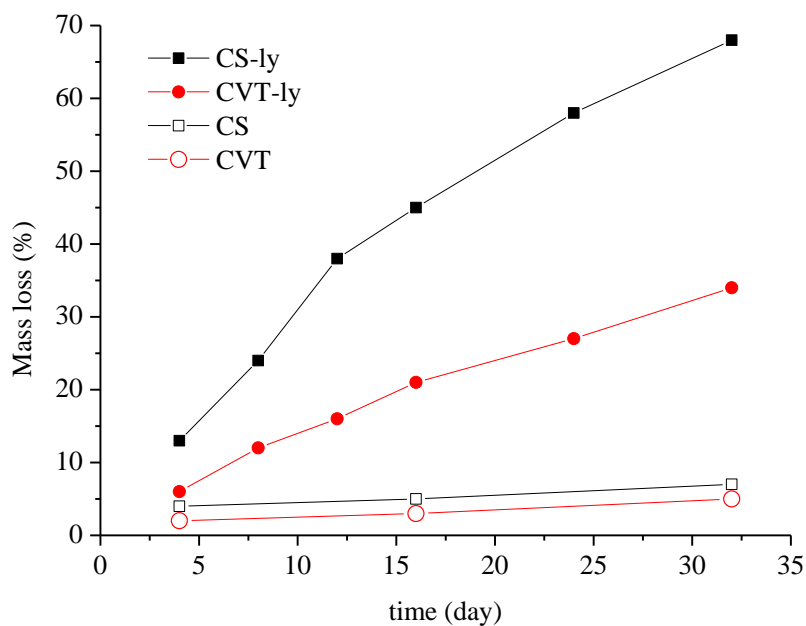
Figure 3.19 weight losses of CVT hydrogel films in 1 mg/ml lysozyme / PBS and in PBS without lysozyme at 37 C as a function of time. Black and red mark shows the sample of with and without lysozyme, respectively.

3.2 Swelling Experiments

3.2.1 Swelling Test

To investigate the time-dependent swelling behavior of Hydrogel films in solutions with different pH, we performed dynamic swelling studies. The swelling S% is calculated from Equation 2.1.

Swelling curves of hydrogel films in solutions with pH=1.2 and pH=7.4 at 37°C were shown in Figures 3.20 A and B, respectively.
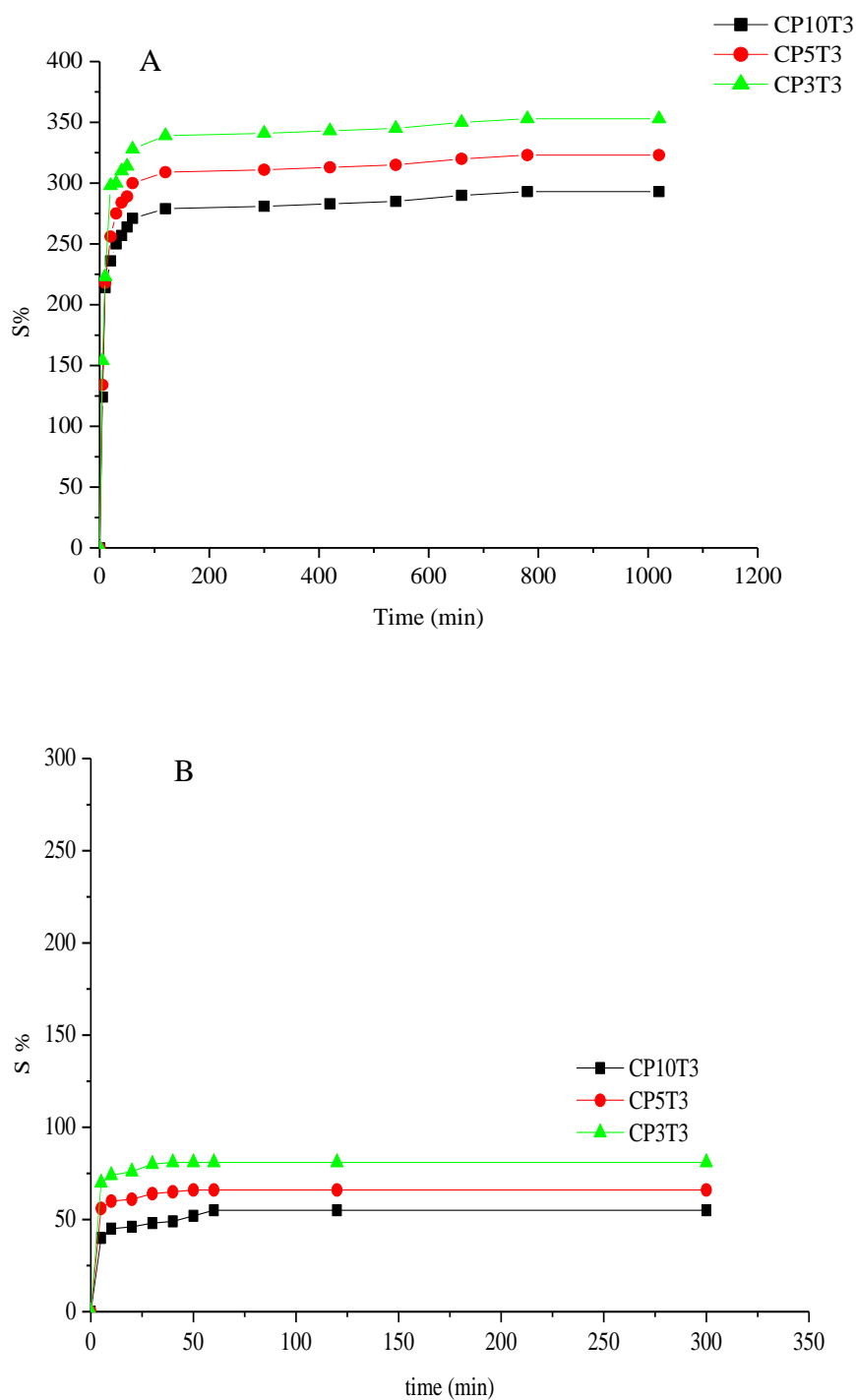
Figure 3.20 Swelling ratio of CPT a) at pH1.2 and b) at pH 7.4 at 37 °C

As can be seen in Figure 3.20, the values of equilibrium swelling of CPT Hydrogels have decreased with increasing PEG concentrations in hydrogels. The swelling degree of a hydrogel depends on its network structure, which is controlled

by the concentration of the crosslinker. Also, the swelling of hydrogels are depended on the pH of the medium.
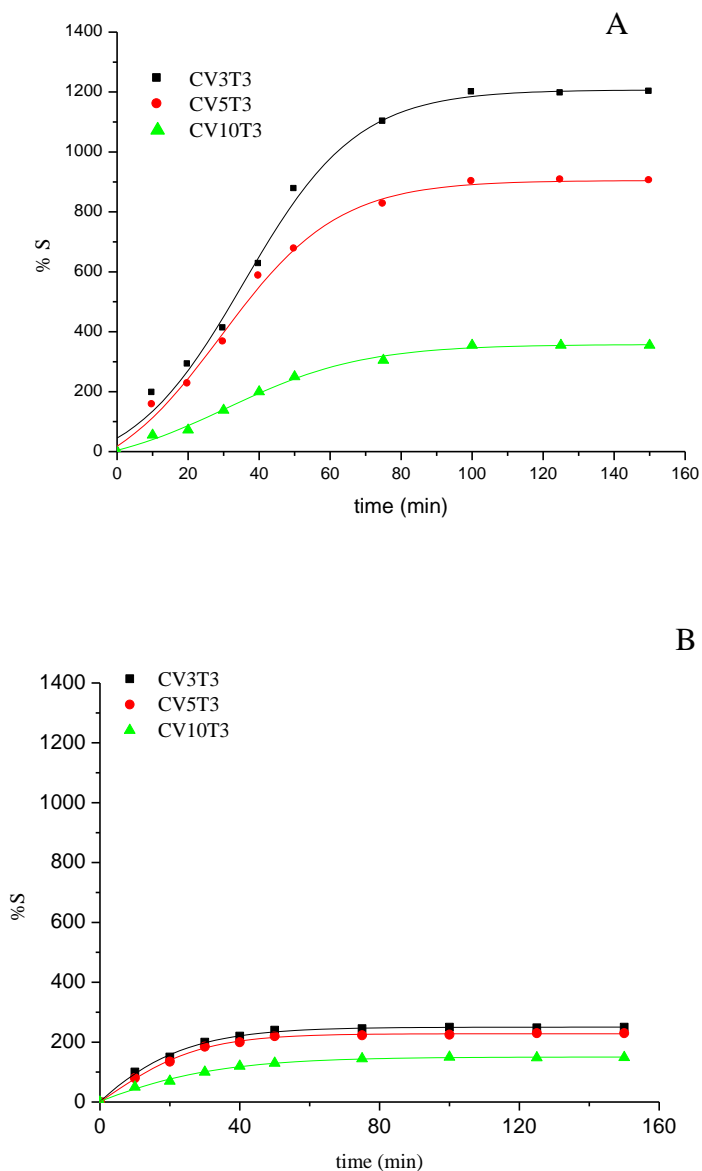

Figure 3.21 Swelling ratio of CVT at A) pH=1.2   B) pH=7.4 at 37°C

As can be seen from in Figure 3.21, the values of equilibrium swelling of CVT Hydrogels have decreased with increasing PVA concentrations in hydrogels. The swelling degree of a hydrogel depends on its network structure, which is controlled by the concentration of the PVA. In addition, hydrogels swelling is based on pH of

medium because of $-NH_2$ groups in Chitosan. On the other hand, the decrease of swelling (%) with the increase of PVA content is due to the high hydrophobicity of PVA.

For extensive swelling of polymers, the following relation can be written as below (Katime, et. al., 2001);

$$\frac{t}{S} = A + Bt \qquad (3.1)$$

where S is the degree of swelling at time t, $B = \dfrac{1}{S_{max}}$ is the inverse of the maximum swelling, $A = \dfrac{1}{(dS/dt)_0} = \dfrac{1}{S_{max}^2 k_s}$ is the reciprocal of the initial swelling rate (r_o) the gel.

Table 3.5 Swelling parameters of CPT at 37°C for different pH values

			pH=7.4	
			k_s x10^5	r_o
Sample	S_{eq} %	S_{max} %	[g CPT (g solution)$^{-1}$s^{-1}]	[g solution (g CPT)$^{-1}$s^{-1}]
CP3T3	81	82	2091	141
CP5T3	66	68	1718	79
CP10T3	55	56	565	18
			pH=1.2	
			k_s x10^5	r_o
Sample	S_{eq} %	S_{max} %	[g CPT (g solution)$^{-1}$s^{-1}]	[g solution (g CPT)$^{-1}$s^{-1}]
CP3T3	323	324	44	46
CP5T3	353	355	42	53
CP10T3	293	295	48	42
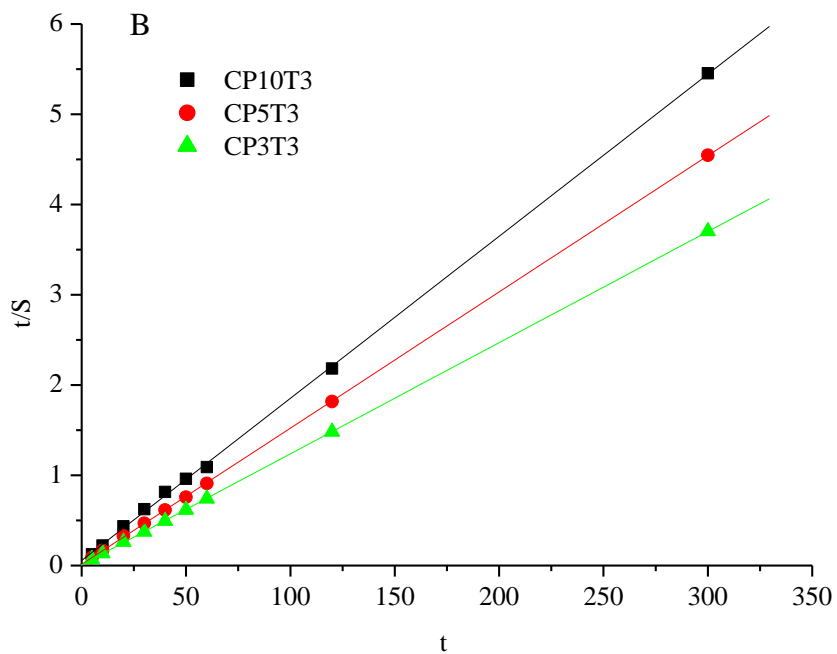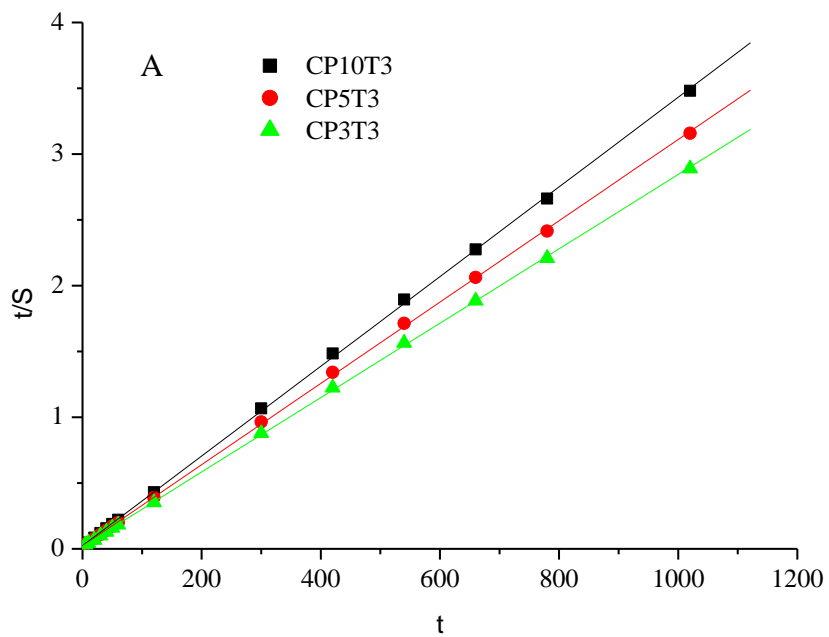
Figure 3.22 Swelling rate curves of CPT Hydrogels A) at pH 1.2 and B) at pH 7.4

The relation represents second-order kinetics. The values of the initial swelling rate, r_o [g solution (g Hydrogel)$^{-1}$s^{-1}] and maximum swelling, S_{max} [g solution (g Hydrogel)$^{-1}$] were calculated from the slope and intersection of the lines and swelling rate constant, k_s [g Hydrogel (g solution)$^{-1}$s^{-1}] were presented in Table 3.5 and 3.6 for CPT and CVT, respectively.
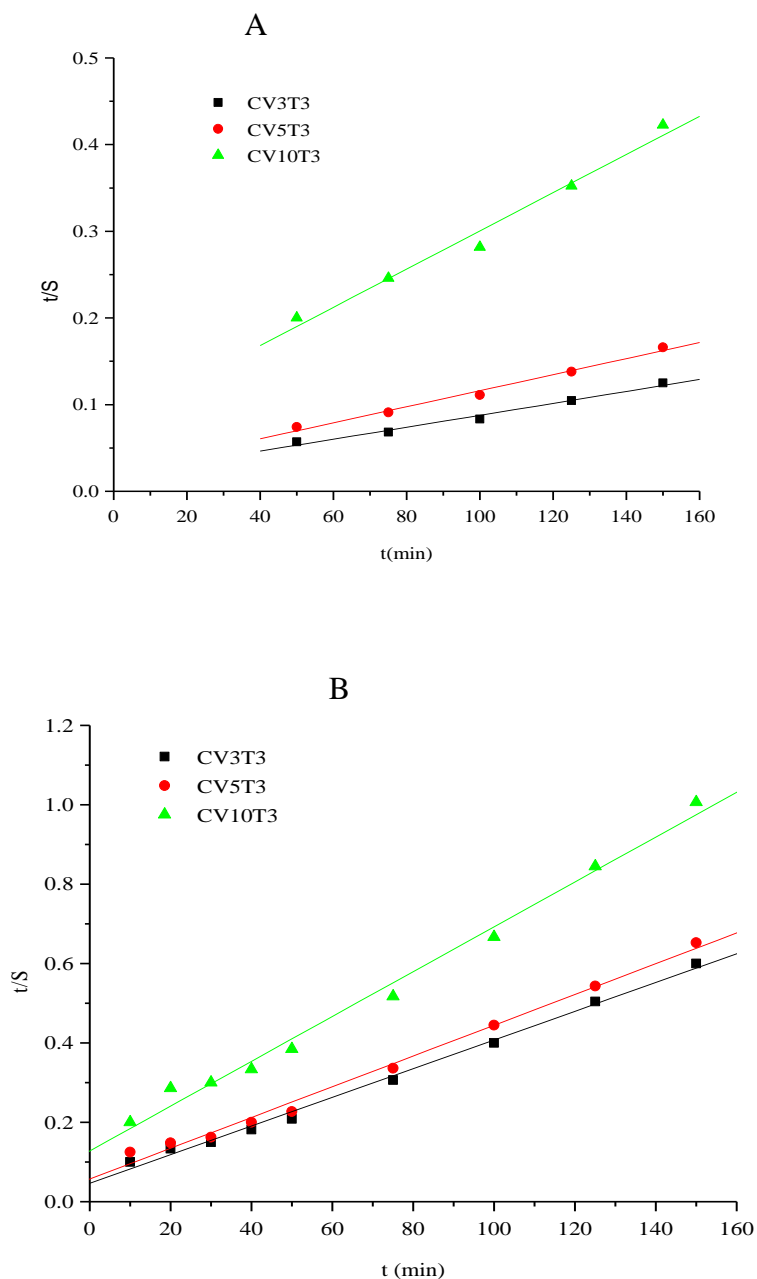

Figure 3.23 Swelling rate curves of CVT Hydrogels A) at pH=1.2 and B) at pH=7.4

Table 3.6 Swelling parameters of CVT at pH=1.2 and 7.4

	pH=7.4			
	S_{eq} %	S_{max} %	$k_s \times 10^4$ [g CVT (g solution)$^{-1}$s^{-1}]	r_o [g solution (g CVT)$^{-1}$s^{-1}]
CV3T3	250	277	2.8	0.046
CV5T3	230	258	2.6	0.057
CV10T3	149	177	2.5	0.130
	pH=1.2			
	S_{eq} %	S_{max} %	$k_s \times 10^4$ [g CVT (g solution)$^{-1}$s^{-1}]	r_o [g solution (g CVT)$^{-1}$s^{-1}]
CV3T3	1200	1452	0.25	0.019
CV5T3	903	1080	0.36	0.023
CV10T3	355	452	0.61	0.080

3.2.2 pH-Sensitivity of Hydrogels

A number of factors that influence the degree of swelling of hydrogel include the properties of the polymer and swelling medium. This is why experiments to determine the pH-dependent swelling kinetics were performed in buffer solutions which have various pH values between 2 and 8, in Figure 3.24 and 3.25 represents the variation of the equilibrium swelling ratio of hydrogel as a function of the pH of the swelling medium at 37°C.

As shown in Figure 3.24, for all the CPT hydrogels, maximum swelling was observed at pH=2 and minimum at pH=6. There was a decrease in the equilibrium swelling ratio of the samples with below pH=6. However, from the pH=6, CPT hydrogel exhibited an increase in equilibrium swelling ratio values. It can be seen

that the hydrogels swelled mostly in acidic medium as compared with the neutral or basic medias.

Whereas, swelling ratio of the samples was decreased with the increasing of the amounts of PEG. On the other hand, the effect of pH on the swelling of the Chitosan hydrogels was explained on the basis of protonation of the amino groups of Chitosan.
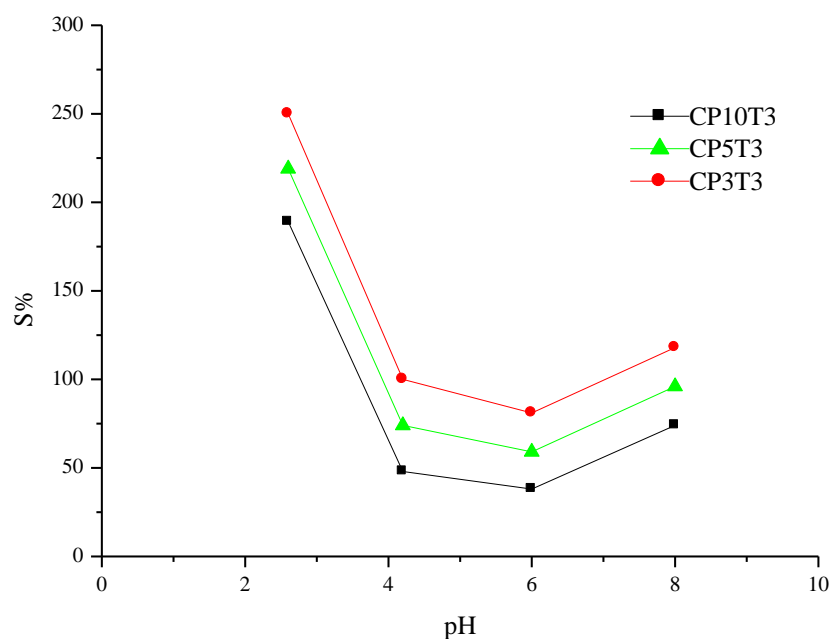

Figure 3.22 Effect of pH on the equilibrium swelling ratio of hydrogel

In the acidic medium, the protonation of the amino groups leads to repulsion in the polymer chains, thus allowing more water in the hydrogel network. At higher pH, deprotonation of the amino groups takes place and repulsion in polymer chains is reduced. This results in the shrinking of the gels and therefore, the amount of water in the gel decreases. Swelling is important properties for drug release study for hydrogel. The sudden and rapid swelling causes degradation and rapid release. At acidic medium, swelling ratio of a gel which 960 percent and 840 percent were synthesized by Ramos et al.; 2006. These hydrogels were broken after the immersion in the soaking phase. However, maximum swelling ratio of the hydrogels was observed as 250 percent, while its minimum was 189 percent in acidic medium. Furthermore, reversible swelling characteristics and low response time of the

samples may be an advantage for drug release study. As can be seen from Figure 3.25, repeated changes in pH for the CPT hydrogels responded reversible pattern with a faster response in swelling than in deswelling.

Figure 3.25 pH dependent reversible swelling behavior of hydrogel (hydrogel sample equilibrated at pH=2.3, then alternated between solutions at pH=8.3 and 2.3).

Figure 3.25 represents the variation of the equilibrium swelling ratio of hydrogel CVT as a function of the pH of the swelling medium at 37 °C. In all the hydrogels, maximum swelling was observed at pH=2 and minimum at pH=8. It can be seen that the hydrogels swelled the mostly in acidic medium compared to the neutral or basic media.

Swelling ratio is proportional to the amount of PVA which increased, swelling is decreasing. The effect of pH on the swelling of the Chitosan hydrogels is explained on the basis of protonation of the amino groups of Chitosan.
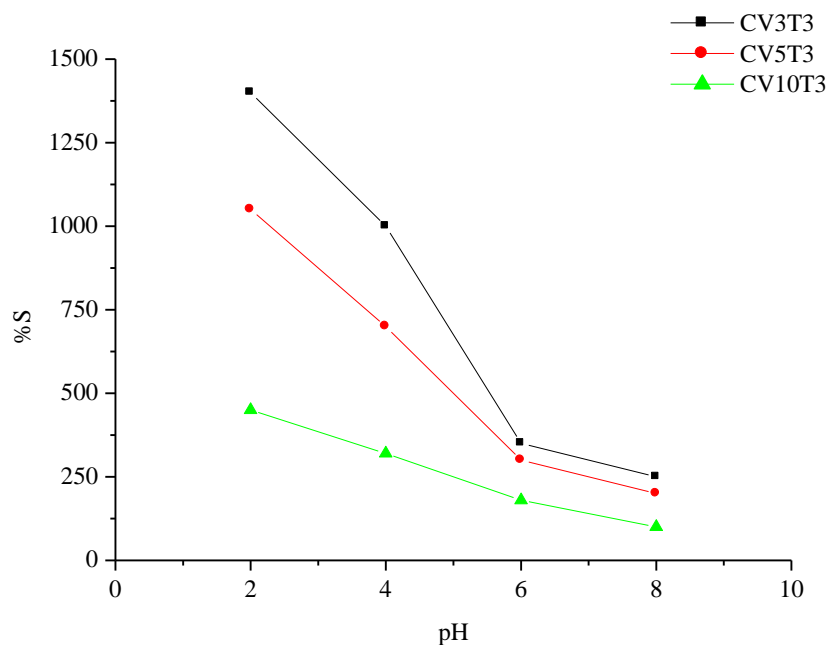
Figure 3.26 Effect of pH on the equilibrium swelling ratio of hydrogel

In the acidic medium, the protonation of the amino groups leads to repulsion in the polymer chains, thus allowing more water in the hydrogel network. At higher pH, deprotonation of the amino groups takes place and repulsion in polymer chains is reduced. This results in the shrinking of the gels and therefore, the amount of water in the gel decreases. Swelling is important properties for drug release study for hydrogel. The sudden and rapid swelling causes degradation and rapid release. Furthermore, reversible swelling characteristic and low response time is an advantage for drug release study. The times of equilibrium were determined 12 and 20 minutes in acidic and basic area, respectively. While there were repeated changes in pH, the CVT hydrogels exhibited a reversible pattern with a faster response in swelling than in deswelling in Figure 3.27.
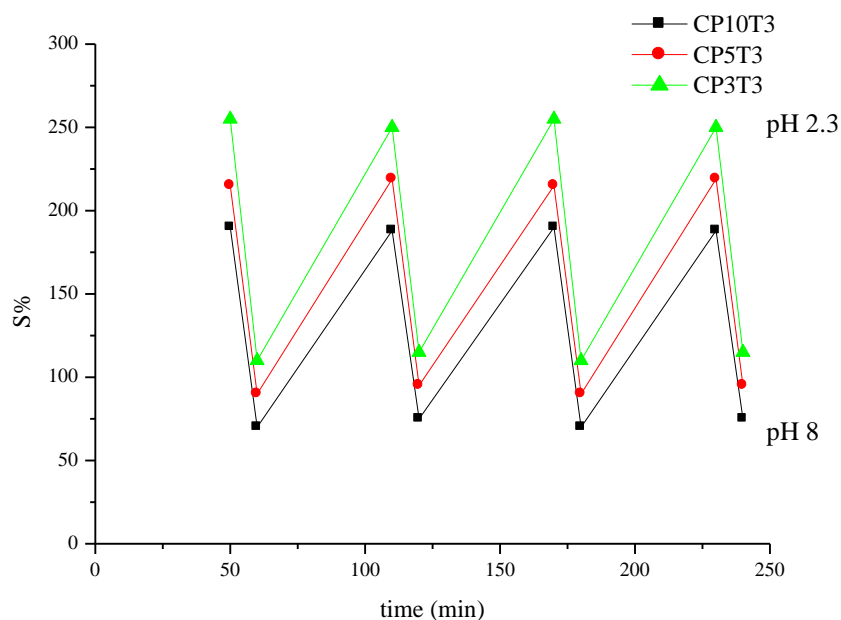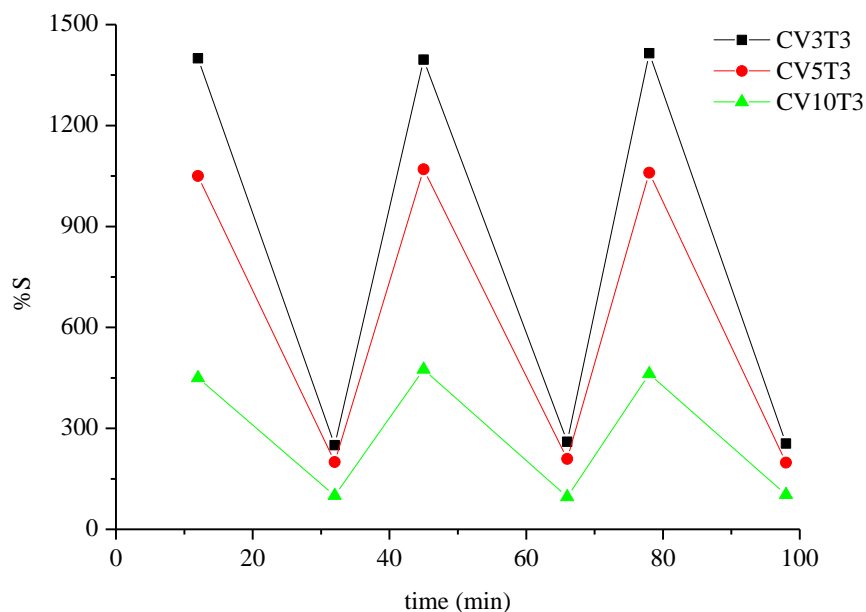
Figure 3.27 pH dependent reversible swelling behavior of hydrogel (hydrogel sample equilibrated at pH=2.3, then alternated between solutions at pH=8 and 2).

3.2.3 Temperature Sensitivity of Hydrogels

Temperature-dependent reversible swelling behaviors of CPT and CVT were found, as shown in Figures 3.28 and 3.29, respectively. At the first run, the equilibrium swelling ratio was measured at 37°C. Then, the equilibrium swelling experiment was done at 4°C for the same film sample. The equilibrium swelling ratio increased with decreasing the temperature to 4°C. When the temperature was raised to 37°C again (3rd run), the equilibrium swelling ratio increased to the level of the first run at 37°C. These heating/cooling runs were repeated two times. The similar reversible and reproducible temperature dependence of swelling–deswelling behavior was observed for all samples.

Figure 3.28 Swelling and deswelling behavior of CPT Hydrogel as a function of time at different temperatures in buffer at pH=7.4
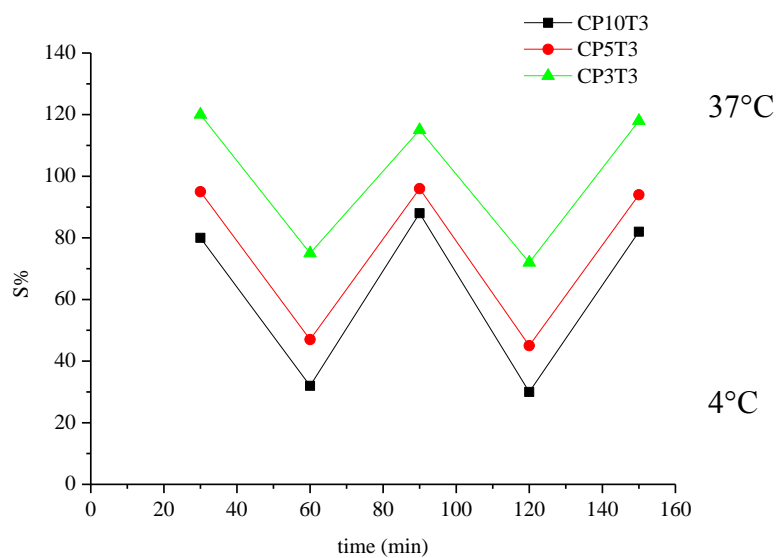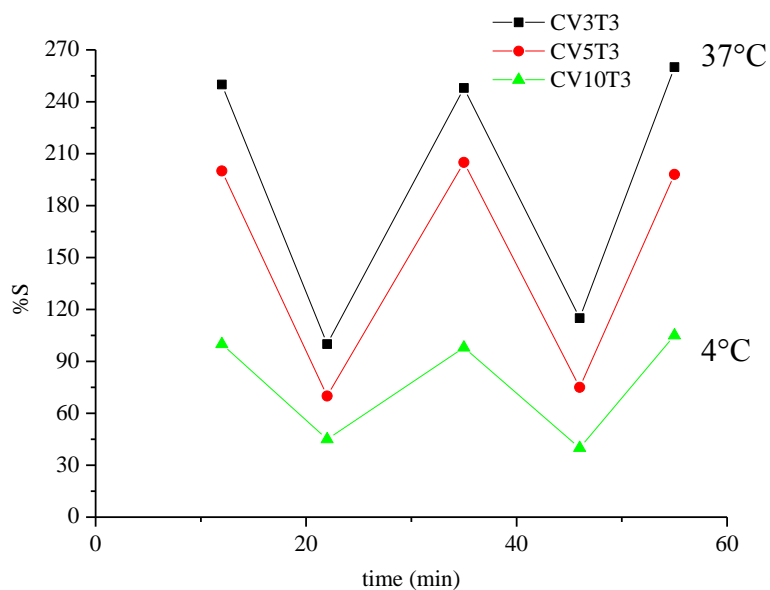

Figure 3.29 Swelling and deswelling behavior of CVT Hydrogel as a function of time at different temperatures in buffer at pH=7.4

Thus, all hydrogel samples have almost the same temperature dependency, higher swelling ratio was observed at higher temperature and lower at lower temperature. It

has been well-known that the swelling–deswelling behavior is mainly due to the interaction between polymer and water molecules.

In general, the strength and extent of this interaction decrease with increasing the temperature. The sample with higher PEG or PVA content was more sensitive to the temperature changes, showing more distinctive temperature-dependent swelling–deswelling response. It would be a desirable character for controlled-drug release system with swelling property controllable by pH and temperature. Therefore, it can be expected that these hydrogel films are of great interest for biomedical application such as artificial muscles or switches and drug delivery systems.

3.3 Application of Hydrogels as Drug Release

3.3.1 Determination of Amoxicillin

3.3.1.1 Standard solutions

Stock solutions of amoxicillin were prepared by dissolving 100 mg of each substance in separate 100 mL calibrated flasks in 2 mL of methanol and completing to volume with distilled water. Further dilutions were made with distilled water to prepare standard solutions containing 10-200 μg mL^{-1} of each drug. The structures of the compounds studied are given in Figure 3.30.
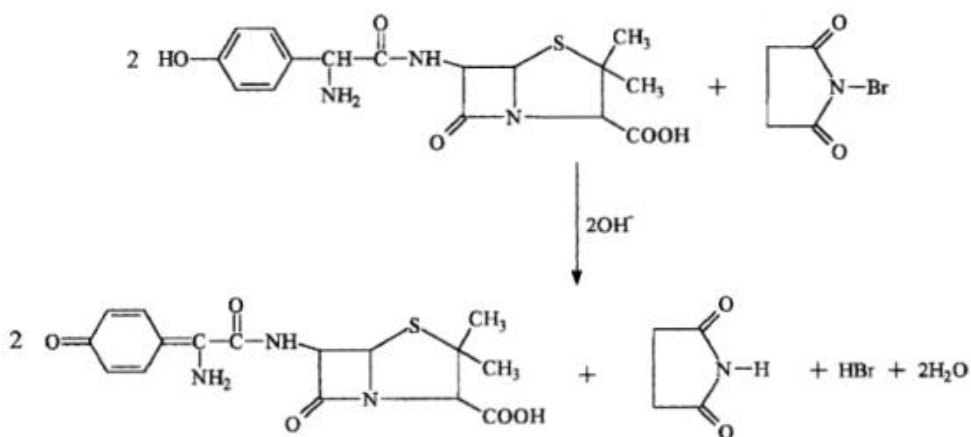

Figure 3.30 Mechanism of amoxicillin oxidation.

The reaction of phenolic compounds with oxidizing agents in alkaline medium is reported to be an oxidation process which consists of the generation of free phenoxy

radicals which can be stabilized by the formation of a quinone through the delocalization of the unpaired electrons over the aromatic ring. This can be achieved by the use of either sodium hydroxide. A possible reaction mechanism is illustrated in Figure 3.30. It is important to mention here that bromination of phenols is expected to occur only in acidic medium (Gamal, 1996).

3.3.1.2 General Procedure

In 10 mL calibrated flasks, place 1.0 mL of the standard drug solution followed by 1.0 mL of 0.1 mol.L^{-1} sodium hydroxides and 0.5-2.5 mL of 0.05-0.1 % *N*-bromosuccinimide (NBS) solution. Mix well, complete to volume with methanol and measure the absorbance at 395 nm against a blank solution prepared similarly.

3.3.1.3 Concentration of NBS

Firstly, concentration of NBS was determined by calibration curve. As shown in Figure 3.31, there was a linear relationship between absorbance and drug concentration (mg/L) at 0.05 % NBS solution with a correlation factor of 0.9987.
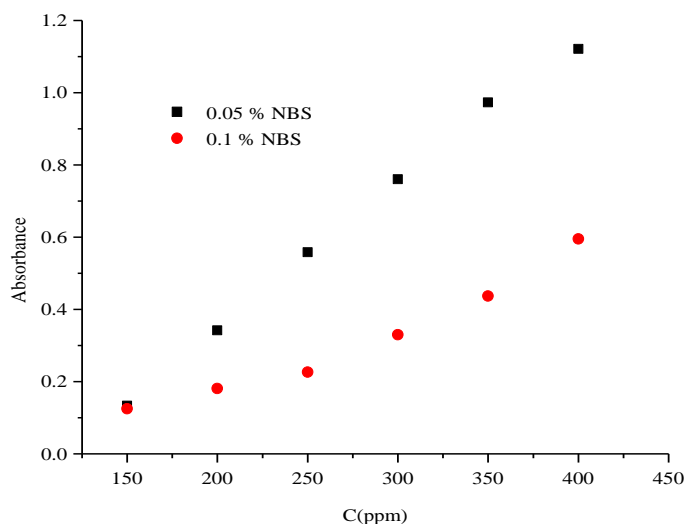

Figure 3.31 Calibration curve with 0.05% NBS and 0.1 % NBS

Increasing concentration of NBS was decreased absorbance and correlation factor (R^2=0.9766). Because of this result, 0.05 % NBS solution was used in all experiment.

3.3.1.4 Volume of the Reagent (NBS)

As shown in Table 3.7, it was found that maximum absorbance values were obtained when 0.75 mL 0.05% NBS solution was used. In addition, correlation factor of calibration curve was affected by added to different volumes of NBS. As indicated in Figure 3.32 and 3.33, the useable volume of NBS was determined as 0.75 mL with correlation factor. This result supported the previous experiments.

Table 3.7 Effect of volume of NBS

V (mL)	Abs. (10ppm)	Abs. (20ppm)	Abs. (30ppm)	Abs. (40ppm)	Final concentration of NBS (%)	R^2
0.25	0.355	0.509	0.564	0.462	1.25×10^{-3}	0.7946
0.5	0.156	*0.612*	0.792	0.92	2.5×10^{-3}	0.9986
0.75	*0.11*	0.399	*1.005*	*1.152*	3.75×10^{-3}	0.9562
1	0.077	0.277	0.762	1.146	5×10^{-3}	0.9406
1.5	0.061	0.193	0.399	0.724	7.5×10^{-3}	0.8609
2	0.047	0.181	0.306	0.615	10×10^{-3}	0.7682
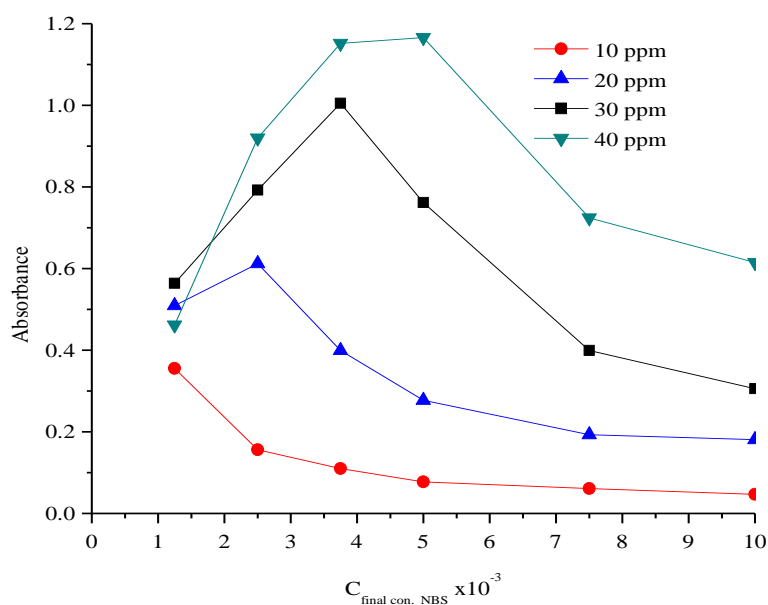
Figure 3.32 The effect of reagent volume
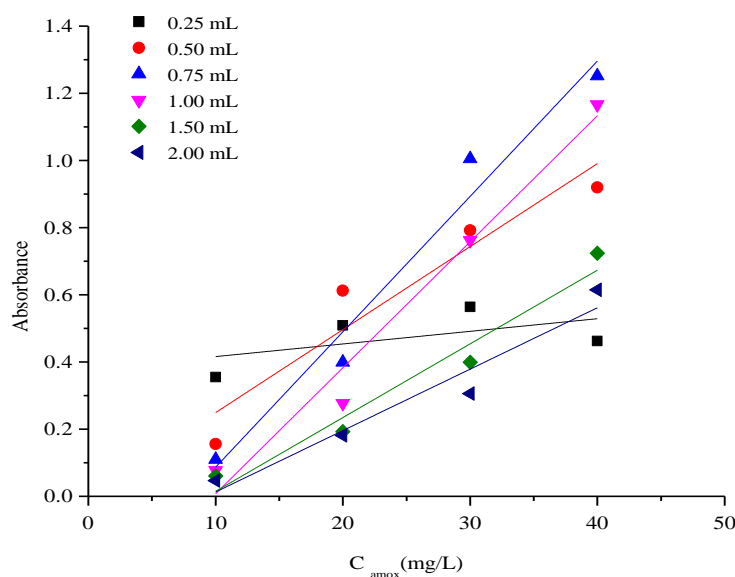
Figure 3.33 Different volumes of NBS

3.3.1.5 Determination of oxidation time for Amoxicillin

Stable structure was determined by completion of the oxidation time with absorbance at 395 nm for different volume of NBS. Oxidation time was detected from 0 to 45 min. Appropriate time of oxidation was found to be 45 min in Figure 3.34.

According to the study, concentration of NBS, volume of NBS and oxidation time were determined as 0.05%, 0.75 mL and 45 min, respectively. The percent cumulative release of amoxicillin from hydrogels to solutions was calculated by Equation 3.2.

The percent cumulative release of amoxicillin from hydrogels to solutions was calculated by:

$$\%R = \frac{M_t}{M_o} \times 100 \tag{3.2}$$

where M_t and M_o are the amount of drug released at time t and in the dry hydrogels, respectively.
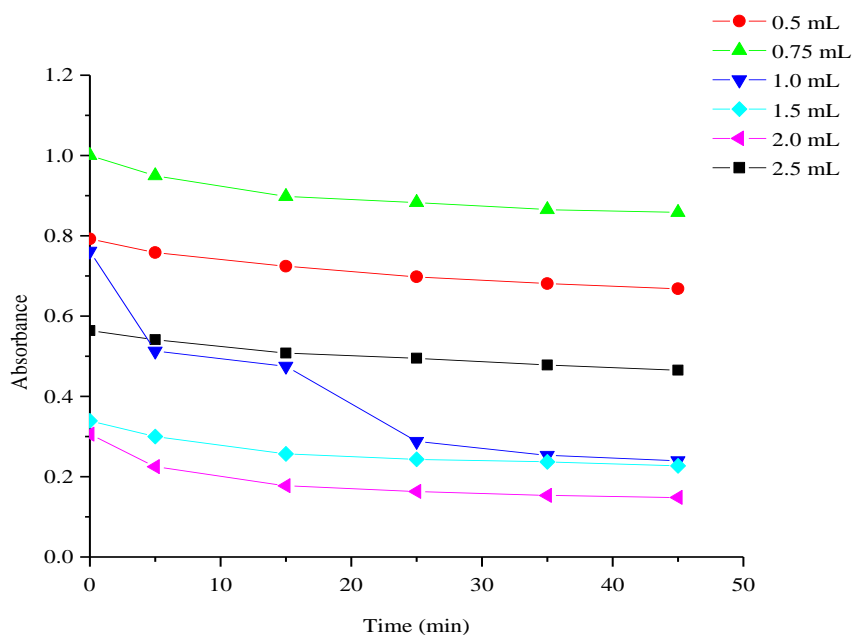
Figure 3.34 Determination of oxidation time at 395 nm by UV spectrophotometer.

3.3.2 Release Studies

3.3.2.1 Kinetic Study

Amoxicillin was selected as our model drug; HCl/KCl solution and Na_2HPO_4-KH_2PO_4 (pH=7.4) solution were used as modulated media. The percent cumulative release of amoxicillin from hydrogels to solutions was calculated by:

$$\%R = \frac{C_t}{C_o} \times 100 \tag{3.3}$$

where C_t and C_o are the amount of drug released at time t and initial amount of amoxicillin in the hydrogels, respectively. To investigate the parameters of release kinetics, Equation (3.4) was used and the plots of t/C_t versus t are presented in Figure 4.30-4.31.

$$\frac{t}{C_t} = \alpha + \beta t \tag{3.4}$$

Here, C_t is the amount of drug released at time t, $\beta = 1/C_{max}$ is the inverse of the maximum amount of released drug, $\alpha = 1/C^2_{max}k_{rel} = 1/r_o$ is the inverse of the initial release rate, and k_{rel} is the constant of the kinetic of release. Figure 3.35 and 3.36 depict the percent cumulative release of amoxicillin from CPT and CVT hydrogels at pH=1.2 and pH=7.4, respectively, at 37°C.

Table 3.8 Release kinetics parameters of CPT and CVT hydrogels in solutions with different pH

	C_{max} (mg)	$k_{(rel)}$ (s^{-n})	r_o (mg s^{-1})
	pH=1.2		
CP3T3	23.5	15×10^{-3}	8.3
CP5T3	26.3	0.95×10^{-3}	0.66
CP10T3	30	0.2×10^{-3}	0.22
	pH=7.4		
CP3T3	18.9	13×10^{-3}	4.7
CP5T3	14.7	2.3×10^{-3}	0.49
CP10T3	7.2	1.6×10^{-3}	0.08
	pH=1.2		
CV3T3	25	4×10^{-3}	2.9
CV5T3	25.5	2.4×10^{-3}	1.5
CV10T3	23.4	1.01×10^{-3}	0.56
	pH=7.4		
CV3T3	13.9	1.96×10^{-3}	0.30
CV5T3	13.8	1.36×10^{-3}	0.26
CV10T3	5.5	1.18×10^{-3}	0.04
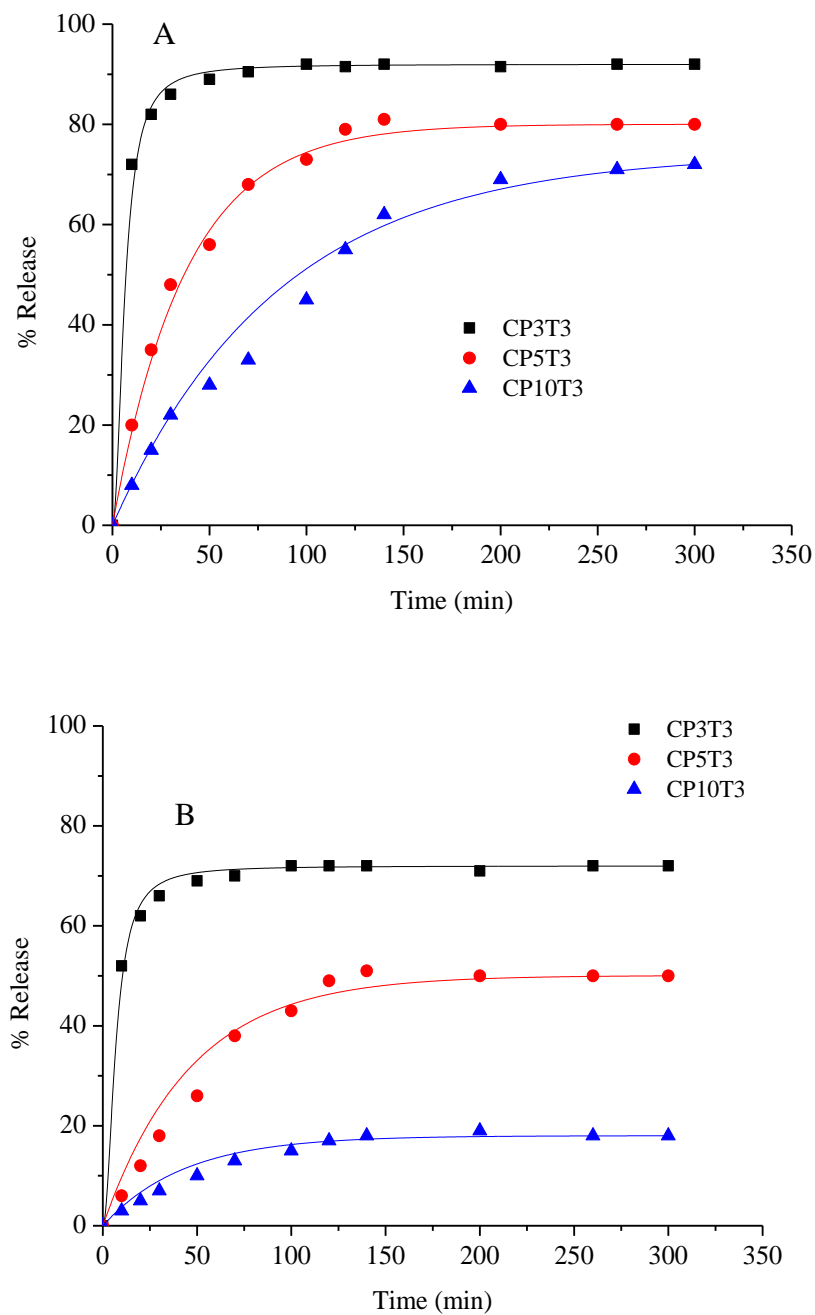
Figure 3.35 Effect of different ratio of PEG on the in vitro release rate
(%) of amoxicillin in A) pH=1.2 and B) pH=7.4
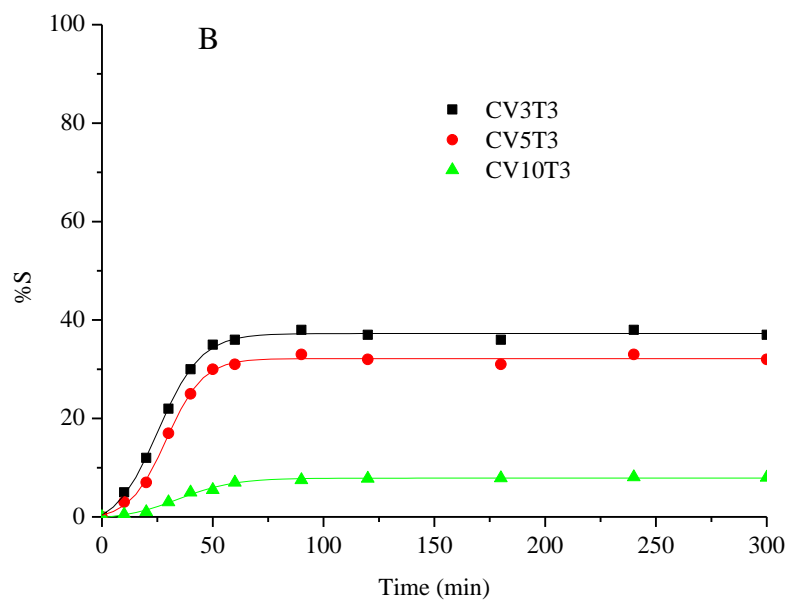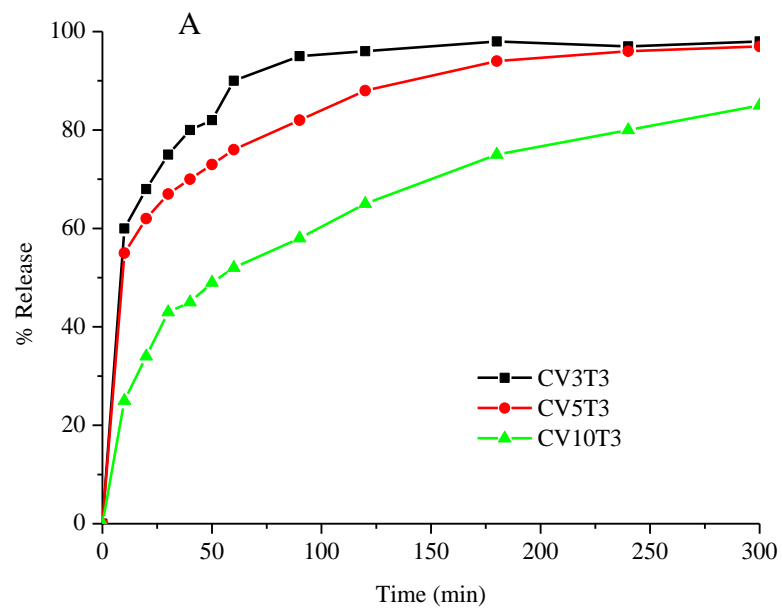
Figure 3.36 Effect of different ratio of PVA on the in vitro release rate (%) of amoxicillin in A) pH=1.2 and B) pH=7.4
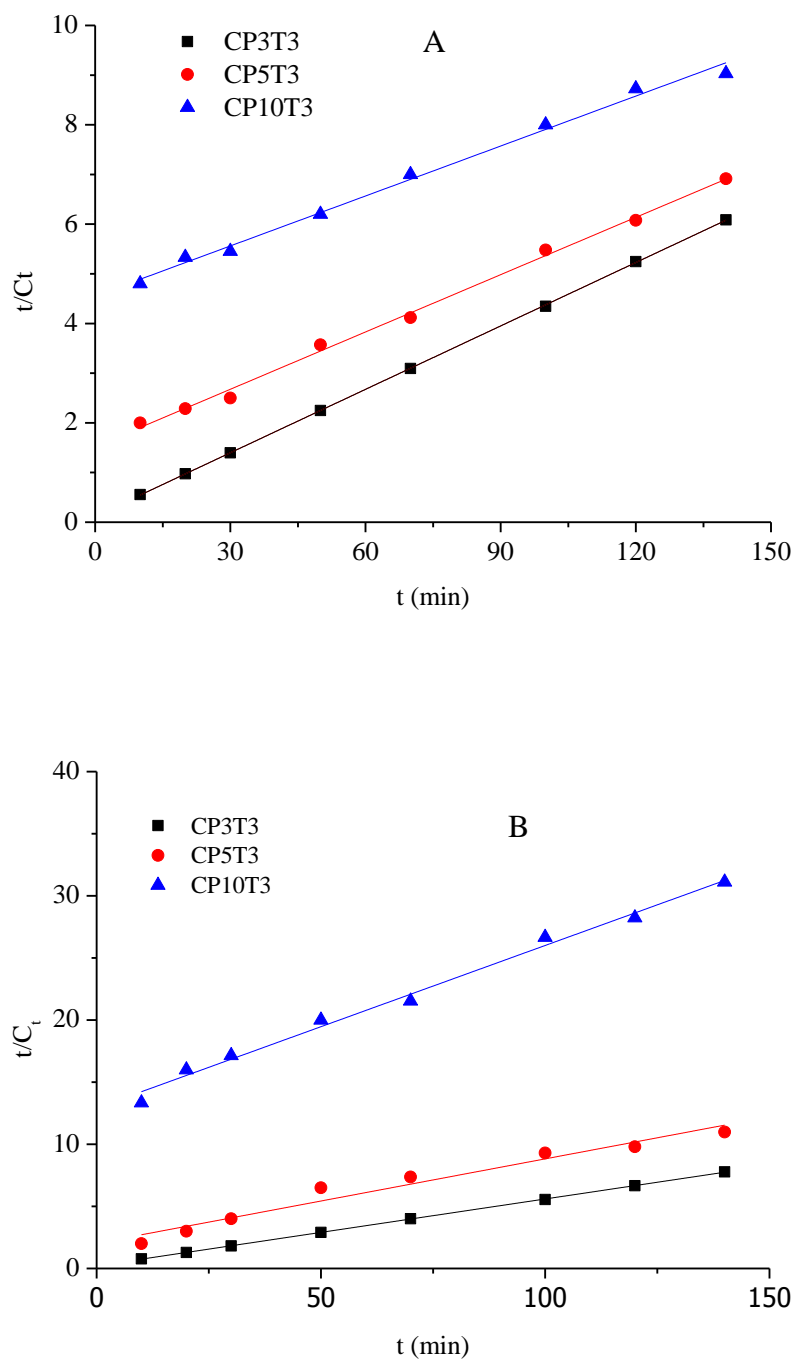
Figure 3.37 Release rate curves of CPT Hydrogel in A) pH=1.2 and B) pH=7.4

Figure 3.35 A-B shows that drug release is pH dependent. The percentage cumulative release of amoxicillin from CPT hydrogels was higher in acidic medium than in the basic medium. On the other hand, change in the amount of PEG was

affected on release rate. Amoxicillin release rate was decreased with increasing amount of PEG.   As shown in table 3.8, it was observed that release results are very similar to swelling results. This parallel behavior is reasonable since drug release from CPT hydrogels into solution is swelling controlled.
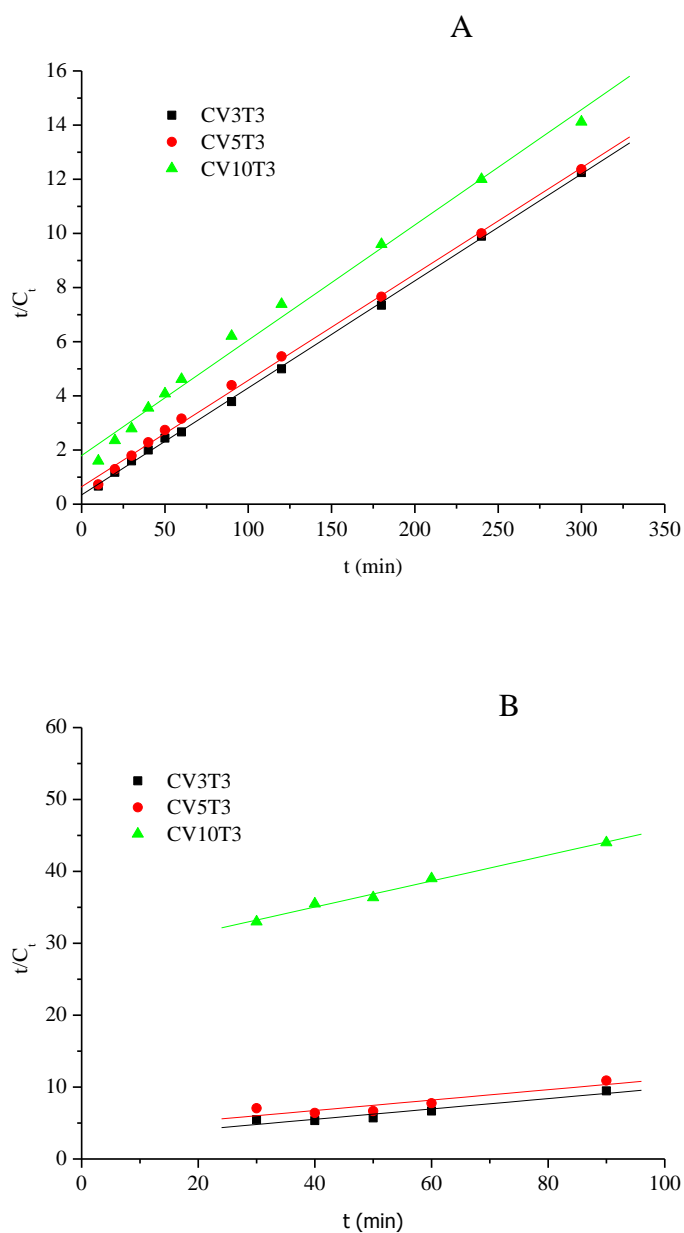
Figure 3.38 Release rate curves of CVT Hydrogel in A) pH=1.2 and B) pH=7.4

3.3.2.2 Diffusion Study

For a successful drug delivery system, it is imperative that one can predict the mechanism of release of the active agent. This is also one of the most challenging fields in drug delivery, and over the years researchers have predicted the release of active drugs as a function of time, using both simple and sophisticated mathematical models. Mathematical models give us an insight into mass transport, as well as the effect of design parameters, such as device geometry and drug loading, on the release mechanism of the active agent in question. These models are important in both the design stage as well as in the experimental verification of the release mechanism (Siepmann & Peppas, 2001). Thus accurate data, along with models accurately representing the data, together provide a valuable insight into the actual release mechanism. Most of the theoretical models found in literature are based on diffusion Equations. Diffusion is a phenomenon largely dependent on the structure of the gel matrix through which it occurs; thus the morphology of the polymeric materials must be taken into account for an accurate model to be selected. Controlled release systems can be categorized based on the rate limiting step and can classified as follows (Peppas, et al., 2000):

- Diffusion-Controlled (drug diffusion from the non-degraded polymer)

- Swelling-Controlled (enhanced drug diffusion due to polymer swelling)

- Chemically Controlled (drug release due to polymer degradation and erosion)

Ordinary diffusion takes place to a certain degree, in each of these mechanisms, thus an understanding of the fundamentals of diffusion, and related mathematical relations are an integral part of understanding the release mechanism of any agent through these gel matrices. For a non biodegradable matrix, drug release occurs due to the concentration gradient either via diffusion or matrix swelling. For biodegradable matrices, release is controlled by the hydrolytic cleavage of polymer chains that lead to matrix erosion (Peppas, et al., 2000). Thus each system has different models which are developed according to the type of release. Simple Equations have been developed for describing drug release of various polymers of different shapes using the principles of diffusion. The diffusion coefficient is defined

in several different ways according to the nature of pores in the system. It is observed that diffusion can be Fickian, anomalous, or Case-II type diffusion. Fickian diffusion and its diffusion coefficient can be easily described using Equations derived from Fick's law and its solutions. Short time approximations of these solutions have been shown to be effective only for the first 60% of drug release, when the aspect ratios are consistent with those of either a flat disk, or a long cylinder.

The following Equation is used to determine the nature of diffusion of buffer solutions into Hydrogels:

$$\frac{C_e}{C_o} = F = kt^n$$

(3.5)

where F is the fractional uptake at time t, k is a constant incorporating characteristic of the macromolecular network system and the penetrant, and n is the diffusional exponent, which is indicative of the transport mechanism.

Table 3.9 Diffusion parameters of CPT Hydrogels at 37°C.

	k(mg/min)	n	R^2
CP5T3 (pH=1.2)	47x 10^{-3}	0.67	0.95
CP5T3 (pH=7.4)	9.4x 10^{-3}	0.84	0.99
CP10T3 (pH=7.4)	6.5x 10^{-3}	0.69	0.99
CP10T3 (pH=1.2)	16x 10^{-3}	0.73	0.98

Fickian diffusion and Case II transport are defined by n valuing to 0.5 and 1, respectively. Anomalous transport behavior (non-Fickian diffusion) is intermediate between Fickian and Case II. That is reflected on n between 0.5 and 1. For the hydrogels, lnF versus lnt graphs are plotted and shown in Figure 3.39 n exponents and k parameters were calculated from the slopes and intercepts of the lines, respectively, and were listed in Table 3.9 which shows that hydrogels presented a

non-Fickian release with n values 0.67- 0.84 but CP3T3 release pattern was not determined.
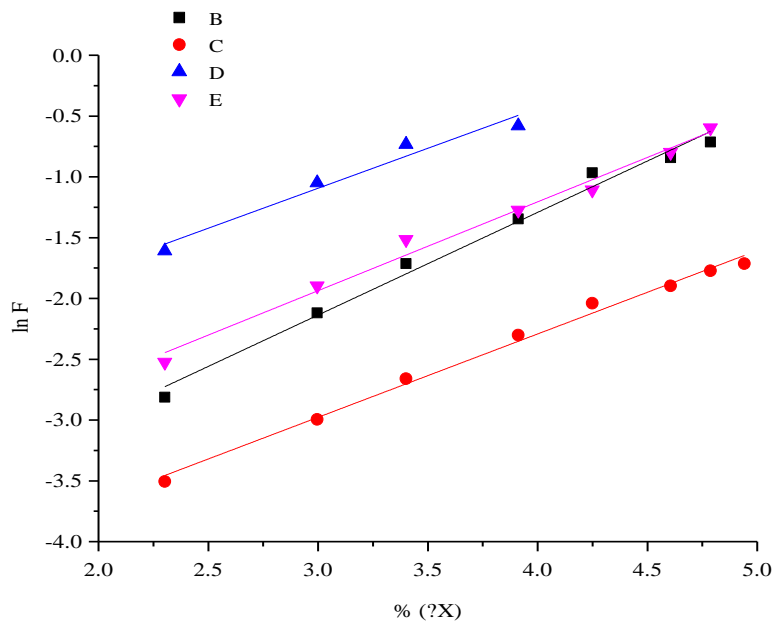
Figure 3.39 Plots of ln F vs lnt of CPT at pH=7.4 and pH=1.2 at 37°C.

For the hydrogels, lnF versus lnt graphs were plotted and shown in Figure 3.40 n exponents and k parameters were calculated from the slopes and intercepts of the lines, respectively, and were listed in Table 3.10 which showed that only CV10T3 hydrogel presented a non-Fickian release with n values 0.38 but other release pattern was not determined.
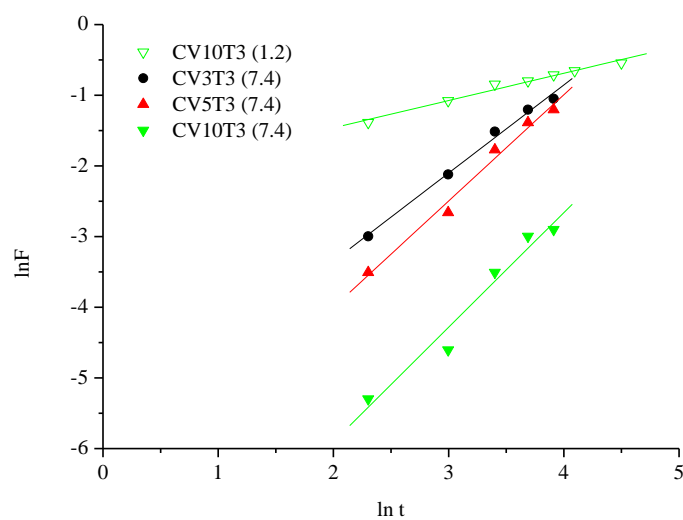
Figure 3.40 Plots of ln F vs lnt of CVT at pH=7.4 and pH=1.2 at 37°C.

Table 3.10 Diffusion parameters of CVT Hydrogels at 37°C.

	k(mg/min)	n	R^2
CV3T3 (pH=7.4)	2.9×10^{-3}	1.25	0.997
CV5T3 (pH=7.4)	0.9×10^{-3}	1.50	0.993
CV10T3 (pH=7.4)	0.12×10^{-3}	1.62	0.981
CV10T3 (pH=1.2)	0.107	0.38	0.990

CHAPTER FOUR

CONCLUSIONS

Hydrogels are three dimensional crosslinked matrices which have recently become one of the most widely used material for biomedical applications. The ability of the gel to absorb biological fluids accounts for its biocompatibility and its use in varied clinical applications, ranging from drug delivery carriers and encapsulation. Drug delivery is one of the most prominent fields of research today, and the development of biocompatible, flexible and strong materials is one of the main concerns. Hydrogels are thus ideal materials for these applications.

In this study, the PEG-TA and PVA-TA cross-linked Chitosan hydrogel films were prepared successfully with different contents of PEG and PVA. Also, they were characterized by FTIR, SEM, XRD, NMR and thermal methods (TGA/DTG and DSC).

FTIR spectra of the samples were shown in Figure 3.1 and 3.2. As can be seen from the Figures that the formation of the cross-linked structure was confirmed by comparing absorption bands of amide I and amide II for all samples.

NMR spectrum of CPT and CVT were shown in Figure 3.3 and 3.6, respectively. While the -CHNH$_2$ peak was disappeared, the peak of -NHCOR was formed. Also, the –R-NHR which was indicated that crosslinked TA.

The surface morphology of hydrogels was investigated with SEM analysis in Figure 3.7 and 3.8. As shown in Figure 3.7a, Chitosan hydrogel have spherical surface morphology but this spherical morphology does not appear in SEM images of crosslinked hydrogel CPT and CVT. The small holes on the surface were disrupted and different structures such as fibrous on CPT hydrogel surface. On the other hand, in CVT hydrogel, after the crosslinking reaction, sphere had become thinner fibers, as shown in Figure 3.8. The crystallinity might be increased with crosslinking as Chitosan hydrogel.

X-ray diffraction patterns of Chitosan, CPT and CVT hydrogel films were indicated in Figure 3.9 and 3.10. The intensity of the characteristic peak of Chitosan 20° was increased with crosslinking. Also, the new peaks were observed at 2θ=10° and 15°. These XRD results were shown an increase at crystalline structure which were also supported in SEM analysis.

The thermal stability of hydrogels was determined with TGA/DTG and DSC thermograms in Figures 3.11 − 3.16. Chitosan has two degradation stages, but CPT and CVT have three degradation stages. By measuring the melting point temperature by DSC in Figure 3.13 and 3.16, the internal three dimensional structure of cross-linked Chitosan hydrogel film was turn out to become dense as the increase of PEG content and as the adding of PVA. The thermal stabilities of the crosslinked Chitosan samples were higher than Chitosan film sample.

As shown in Figure 3.17 and 3.19, there were differences between enzymatic degradation of CPT and CVT hydrogels, because of the different crystal form. According to Figure 3.17, the CPT hydrogel film with higher content of PEG was more sensitive to the enzymatic degradation compared with Chitosan hydrogel film. However, in that CVT hydrogel film were broken down more slowly according to the Chitosan film. These results were showed that the crosslinking of Chitosan with PEG and PVA had been different form.

Swelling properties of the hydrogels were studied at different temperatures as well as in media of different pH values. As shown in Figure 3.20 to3.23, swelling properties of hydrogels were depended on pH and amount of crosslinker. The swelling ratio increased with the decrease of pH value of the surrounding buffer solution.

All films also showed similar reversible temperature-dependent swelling behavior and the high swelling ratio at high temperatures. The swelling rate would be controllable by changing the content of PEG and PVA. In addition, reversible swelling properties were demonstrated that these hydrogels might be pH sensitive system.

Finally, as a drug delivery experiments in vitro release of amoxicillin from CPT and CVT Hydrogels were studied. It has been found that the hydrogels of lower content of crosslinker show the highest degree of swelling and release rate. Also the release behavior of amoxicillin from the hydrogel was very sensitive with at the pH of medium. It has been also determined that release of amoxicillin was very high at pH= 1.2.

Although CPT Hydrogels have most sensitivity but release rate of CVT hydrogels have much more slowly so that CVT hydrogels can lead to a successful application for localized drug delivery used for stomach.

In future, one should also study with PVA type hydrogels which will be cross-linked different ratios of tartaric acids.

The originality of the work was realized with the use of tartaric acid as a natural cross linker which contains binary acidic functional groups.

REFERENCES

Bailey, F.E. & Koleske, J.V. (1976). Poly(Ehtylene Oxide). *Academic Press*, New York,

Bajpai, A.K., Sandeep, K. S., Smitha, B., & Kankane, S. (2008). Responsive polymers in controlled drug delivery. *Progress in Polymer Science,* 33, 11, 1088-1118.

Bardonnet, P. L., Faivre, V., Pugh, W. J., Piffaretti, J. C. & Falson, F. (2006). Gastroretentive dosage forms: Overview and special case of Helicobacter pylori. *Journal of Controlled Release*, 111, 1.

Bebu, A., Szabo, L., Leopold, N., Berindean, C., & David, L. (2011). IR, Raman, SERS and DFT study of amoxicillin. *Journal of Molecular Structure*, 993 52–56.

Bhattarai, N., Gunn, J., & Zhang M. (2010). Chitosan-based hydrogels for controlled, localized drug delivery. *Advanced Drug Delivery Reviews*, 62, 83–99.

Bhattarai, N., Ramay, H. R., Gunn, J., Matsen, F. A., & Zhang, M. (2005). PEG-grafted Chitosan as an injectable thermosensitive hydrogel for sustained protein release. *Journal of Controlled Release,* 103, 609–624.

Bouwstra, J. A. & Junginger, H. E. (1993). *Hydrogels. In Encyclopaedia of Pharmaceutical Technology,* 441-465.

Brugnerotto, J., Lizardi, J., Goycoolea, F. M., Monal, W. A., Desbrières, J., & Rinaudo, M. (2001). An infrared investigation in relation with chitin and chitosan characterization. *Polymer*, 42, 3569–3580.

Cao, W., Cheng, M., Ao, Q., Gong, Y., Zhao, N., & Zhang, X. (2005). Physical, mechanical and degradation properties, and Schwann cell affinity of crosslinked Chitosan films. *Journal of Biomaterials Science–Polymer Edition*, 16, 791–807.

Censi, R. (2010). Temperature Sensitive Hydrogels for Protein Delivery and Tissue Engineering. *University of Utrecht*, Italy.

Christopher, S.B., & Peppas, N.A. (1996). Pulsatile local delivery of thrombolytic and antithrombotic agents using poly(N-isopropylacrylamide-comethacrylic acid) hydrogels. *Journal of Controlled Release*, 39, 57–64.

Chun, M.K., Sah, H. & Choi, H.K. (2005). Preparation of mucoadhesive microspheres containing antimicrobial agents for eradication of H. pylori. *International Journal of Pharmaceutics*, 297, 172-179.

Costa, H. S., Mansur, A. A. P., Barbosa, S. E. F., Pereira, M. M., & Mansur, H. S. (2008). Morphological, mechanical and biocompatibility characterization of macroporous alumina scaffolds coated with calcium phosphate/PVA. *Journal Materials Science*, 43, 510–524.

Costa, V. C., Costa, H. S., Oréfice, R. L., & Mansur, H. S. (2007). Preparation of hybrid biomaterials for bone tissue engineering. *Materials Research*, 10, 21–26.

Dung, P., Milas, M., Rinaudo, M., & Desbrieres, J. (1994). *Water soluble derivatives obtained by controlled chemical modifications of Chitosan*. CERMA V-CNRS, B.P. 53 X. 38041 Grenoble Cedex, France.

Ebara, M., Yamato, M., Hirose, M., Aoyagi, T., Kikuchi, A., & Sakai, K. (2003). Copolymerization of 2-carboxyisopropylacrylamide with N-isopropylacrylamide accelerates cell detachment from grafted surfaces of reducing temperature. *Biomacromolecules*, 4, 344–349.

Etienne, O., Schneider, A., Taddei, C., Richert, L., Schaaf, P. & Voegel, C. J. (2005). Degradability of polysaccharide multilayer films in the oral environment: An in vitro and in vivo study. *Biomacromolecules*, 6, 726–733.

Ezequiel, S.C.J., Edel, F. B.S., Alexandra, A.P.M., Wander, L. V., & Herman, S. M. (2009). Preparation and characterization of Chitosan/poly(vinyl alcohol) chemically crosslinked blends for biomedical applications. *Carbohydrate Polymers,* 76, 472–481.

Freier, T., Koh, H.S., Kazazian K. & Shoichet, M.S. (2005). Controlling cell adhesion and degradation of Chitosan films by *N*-acetylation. *Biomaterials*, 26, 5872–5878.

Gamal, A. S. (1996). Two selective spectrophotometric methods for determination of amoxicillin and cefadroxil. *Analyst*, 121, 641-645.

Geismann, C. & Ulbricht, M. (2005). Photoreactive functionalization of poly(ethylene terephthalate) track-etched pore surfaces with 'smart' polymer systems. *Macromolecular Chemistry and Physics*, 206, 268–81.

George, M. & Abraham, T.E. (2007). pH sensitive alginate-guar gum hydrogel for the controlled delivery of protein drugs. *International Journal of Pharmaceutics*, 335 (1-2), 123-129.

Gimenez, V., Reina, J.A., Mantecon, A., & Cadiz, V. (1999), Unsaturated modified poly(vinyl alcohol). Crosslinking through double bonds. *Polymer*, 40, 2759-1767.

Graham, N.B. (1998). Hydrogels: their future, Part I. *Med Device Technol,* 9, 18-22.

Greenwald, R. B., Gilbert, C. W., Pendri, A., Conover, C. D., Xia, J. & Martinez, A. (1996). Drug Delivery Systems: Water Soluble Taxol 2-Poly(ethylene glycol) Ester Prodrugs Design and *in Vivo* Effectiveness. *Journal of Medicinal Chemistry*. 39, 424-431.

Gupta, P., Vermani, K., & Garg, S. (2002). Hydrogels: from contolled release ro pH-responsive drug delivery. *Drug Discovery Today*, 7, 569-579.

Hodge, R.M, Edward, G.H & Simon, G.P. (1996). Water absorption and states of water in semicrystalline poly(vinyl alcohol) films. *Polymer,* 37, 1371-1376.

Ji, H., Mourad, H., Fried, E., & Dolbow, J. (2006). Kinetics of thermally induced swelling of hydrogels. *International Journal of Solids and Structures*, 43, 1878-1907.

Katime, I., Valderruten, N., & Quintana, J. R. (2001). Controlled release of aminophylline from poly(N-isopropylacrylamide-co-itaconic acid) hydrogels. *Polymer International.* 50, 869–874.

Kim, S. W., Bae, Y. H., & Okano, T. (1992). Hydrogels: swelling, Drug Loading and Release, *Pharmaceutical Research,* 9, 283-290.

Kolhe, P. & Kannan, R., M. (2003). Improvement in ductility of Chitosan through blending and copolymerization with PEG: FTIR investigation of molecular interactions, *Biomacromolecules* 4, 173–180.

Kong, X.Y., Li, X.Y., Wang, X.H., Liu, T.T., Gu, Y.C., Guo, G., Luo, F., Zhao, X. Wei, Y.Q. & Qian, Z.Y. (2010). Synthesis and characterization of a novel MPEG–Chitosan diblock copolymer and self-assembly of nanoparticles. *Carbohydrate Polymers,* 79, 170–175.

Kucuk, I. & Kuyulu, A. (2005). Separation behavior of pH sensitive gels in various mixtures. *Proceeding of the 8th polymers for advanced technologies international symposium,* 1–3.

Kurita, K. (2001). Controlled functionalization of the polysaccharide chitin, *Progress in Polymer Science.* 26, 1921–1971.

Langer, R. & Peppas, N.A. (2003). Advances in biomaterials, drug delivery and bionanotechnology. *AIChE Journal*, 49, 2990–3006.

Lin, C.C., & Metters, A.T. (2006). Hydrogels in controlled release formulations: Network design and mathematical modeling. *Advanced Drug Delivery Reviews*, 58, (12-13), 1379-1408.

Liu, S.Q., Yang, Y.Y., Liu, X. M., & Tong, Y.W. (2003). Preparation and characterization of temperature-sensitive poly(N-isopropylacrylamide)-b-poly(D,L-lactide) microspheres for protein delivery. *Biomacromolecules,* 4, 1784–93.

Mansur, H. S., Sadahira, C. M., Souza, A. N., & Mansur, A. A. P. (2008). FTIR spectroscopy characterization of poly (vinyl alcohol hydrogel with different hydrolysis degree and chemically crosslinked with glutaraldehyde. *Materials Science and Engineering C*, 28, 539–548.

Mansur, H. S., & Costa, H. S. (2008). Nanostructured poly(vinyl alcohol)bioactive glass and poly(vinyl alcohol)/chitosan/bioactive glass hybrid scaffold for biomedical application. *Chemical Engineering Journal*, 137, 72–83.

Muhlebach, A., Muller, B., Pharisa, C., Hofmann, M., Seiferling, B., & Guerry, D. (1997). New water-soluble photo crosslinkable polymers based on modified poly(vinyl alcohol). *Journal of Polymer Science, Part A*. 35, 3603-3611.

Nagahara, N., Akiyama, Y., Nakao, M., Tada, M., Kitano, M. & Ogawa, Y. (1998). Mucoadhesive Microspheres Containing Amoxicillin for Clearance of Helicobacter pylori. Antimicrob. *Agents Chemother*. 42, 2492-2494.

Neamnark, A., Sanchavanakit, N., Pavasant, P., Bunaprasert, T., Supaphol P. & Rujiravanit, R. (2007). In vitro biocompatibility evaluations of hexanol Chitosan film. *Carbohydrate Polymers*, 68, 166–172.

Nordtveit, R.J., Varum, K.M., & Smidsrod, O. (1994). Degradation of fully water-soluble, partially N-acetylated Chitosans with lysozyme. *Carbohydrate Polymers*, 23, 253–260.

Nordtveit, R.J., Varum, K.M., & Smidsrod, O. (1996). Degradation of partially *N*-acetylated Chitosans with hen egg white and human lysozyme. *Carbohydrate Polymers*, 29, 163–167.

Ogawa, K., Yui, T., & Okuyama, K. (2004). Three D structures of Chitosan. *International Journal of Biological Macromolecules*, 34, 1–8.

Pangburn, S.H., Trescony, P.V., & Heller, J. (1982). Lysozyme degradation of partially deacetylated chitin, its films and hydrogels. *Biomaterials,* 3,105–108.

Park, H., & Park, K. (1996). Hydrogels in Bioapplications. In Hydrogels and Biodegradable Polymers for Bioapplications. *ACS Symposium Series,* 627, 2-10.

Park, J. S., Park, J.W., & Ruckenstein, E. (2001). Thermal and dynamic mechanical analysis of PVA/MC blend hydrogels. *Polymer*, 42, 9, 4271-4280.

Patel J.K., & Patel M.M. (2007), Stomach Specific Anti-Helicobacter Pylori Therapy: Preparation and Evaluation of Amoxicillin-Loaded Chitosan Mucoadhesive Microspheres. *Current Drug Delivery*, 4, 41-50.

Patel, J.K, & Chavda, J.R. (2009). Formulation and evaluation of stomach-specific amoxicillin-loaded carbopol-934P mucoadhesive microspheres for anti-Helicobacter pylori therapy. *Journal of Microencapsulation*, 26, 365-376.

Peppas, N. A. (1987). Hydrogels in Medicine and Pharmacy. Volumes I-III.*, CRC Press,* Boca Raton, F L,

Peppas, N.A. & Khare, A.R. (1993). Preparation, structure and diffusional behavior of hydrogels in controlled release. *Advanced Drug Delivery Reviews*, 11(1-2), 1-35.

Peppas, N.A., Bures, P., Leobandung, W., & Ichikawa, H. (2000). Hydrogels in pharmaceutical formulations. *European Journal of Pharmaceutics and Biopharmaceutics*, 50(1), 27-46.

Plunkett, K.N., Berkowski, K.L., & Moore, J.S. (2005). Chymotrypsin responsive hydrogels: application of a disulfide exchange protocol for the preparation of methacrylamide containing peptides. *Biomacromolecules*, 6, 632–637.

Properties of tartaric acid. (n.d.). Retrieved May 14, 2011, from http://www.ehow.com/list_6388695_properties-tartaric-acid.html.

Qin, C., Du, Y., Zong, L., Zeng, F., Liu, Y., Zhou, B. (2003). Effect of hemicellulase on the molecular weight and structure of Chitosan. *Polymer Degradation and Stability*, 80, 3, 435-441.

Qu, X., Wirsen, A. & Albertsson, A.C. (2000). Novel pH-sensitive Chitosan hydrogels: swelling behavior and states of water. *Polymer* 41, 4589–4598.

Ramos, M., Rodríguez, N.M., Henning, I., Díaz, M.F., Monachesi, M.P., Rodríguez, M.S., Abarrategi, A., Correas-Magan, V., Lo´pez-Lacomba, J.L., & Agullo, E. (2006), Poly(ethylene glycol) crosslinked N-methylene phosphonic Chitosan. Preparation and characterization. *Carbohydrate Polymers*, 64, 328–336.

Rao, K. S. V. K., Naidu, B. V. K., Subha, M. C. S., Sairam, M., & Aminabhavi, T. M. (2006). Novel chitosan-based ph-sensitive interpenetrating network microgels for the controlled release of cefadroxil. *Carbohydrate Polymers*, 66, 333–344.

Rao, K. V. R., & Devi, K. P. (1988). Swelling controlled-release systems: recent developments and applications. *International Journal of Pharmaceutics,* 48, 1–13.

Rokhade, A. P., Patil, S. A., & Aminabhavi, T. M. (2007). Synthesis and characterization of semi-interpenetrating polymer network microspheres of acrylamide grafted dextran and chitosan for controlled release of acyclovir. *Carbohydrate Polymers*, 67, 605–613.

Russell, R.J., Axel, A.C., Shields, K.L. & Pishko, M.V. (2001). Mass transfer in rapidly photopolymerized poly(ethylene glycol) hydrogels used for chemical sensing. *Polymer,* 42, 4893-4901.

Schilli, C.M., Zhang, M., Rizzardo, E., Thang, S.H., Chong, Y.K., & Edwards, K. (2004). A new double-responsive block copolymer synthesized via raft polymerization, Poly (N-isopropyl acrylamide)-β-poly (acrylic acid). *Macromolecules,* 37, 7861–7866.

Schmoljohann, D., Oswald, J., Jorgensen, B., Nitschke, M., Beyerlein, D., & Werner, C. (2003). Thermo-responsive PNIPAAm-g-PEG films for controlled cell detachment. *Biomacromolecules,* 4, 1733–1739.

Shiga, T., Hirose, Y., Okada, A., & Kurauchi, T. (1992). Electric field associated deformation of polyelectrolyte gel near a phase transition point. *Journal of Applied Polymer Science*, 46, 635–40.

Shigemasa, Y., Matsuura, H., Sashiwa, H., & Saimoto, H. (1996). Evaluation of different absorbance ratios from infrared spectroscopy for analyzing the degree of deacetylation in chitin. *International Journal of Biological Macromolecules*, 18, 237–242.

Shigemasa, Y., Matsuura, H., Sashiwa, H., & Saimoto, H. (1996). Evaluation of different absorbance ratios from infrared spectroscopy for analyzing the degree of deacetylation in chitin. *International Journal of Biological Macromolecules*, 18, 237–242.

Siepmann, J. & Peppas, N.A. (2001). Modeling of drug release from delivery systems based on hydroxypropyl methylcellulose (HPMC). *Advanced Drug Delivery Reviews,* 48, 139-157.

Song, S. Z., Kim, S. H., Cardinal, J. R., & Kim, S.W. (1981). Progestin permeation through polymer membranes, V. Progestrone release from monolthic hydrogel devices. *Journal of Pharmaceutical Sciences.* 70, 216-219.

Sood, A., & Panchagnula, R. (1998). Drug Release evaluation of diltiazem CR preparations. *International Journal of Pharmaceutics* 175, 95-107.

Sugimoto, M., Morimoto, M., Sashiwa, H., Saimoto, H., & Shigemasa, Y. (1998). Preparation and characterization of water-soluble chitin and Chitosan derivatives. *Carbohydrate Polymers*, 36, 49–59.

Suh, J. K. F., & Matthew, H. W. T. (2000). Application of chitosan-based polysaccharide biomaterials in cartilage tissue engineering: A review. *Biomaterials,* 21, 2589–2598.

Tanuma, H., Kiuchi, H., Kai, W., Yazawa, K., & Inoue, Y. (2009). Characterization and enzymatic degradation of PEG-Cross-Linked Chitosan Hydrogel Films. *Journal of Polymer Science,* 114, 1902-1907.

Tanuma, H., Saito, T., Nishikawa, K., Dong, T., Yazawa, K., & Inoue, Y. (2010). Preparation and characterization of PEG-cross-linked Chitosan hydrogel films with controllable swelling and enzymatic degradation behavior. *Carbohydrate Polymers*, 80, 260-265.

Teng, D.V., W.U., Z.M., Zhang, X., Wang, Y.X., Zheng, C., Wang, Z., & Li, C.X. (2010). Synthesis and characterization of in situ cross-linked hydrogel based on self-assembly of thiol-modified Chitosan with PEG diacrylate using Michael type addition. *Polymer,* 51, 639–646.

Torre, D.L., P. M., Enobakhare Y., Torrado G. & Torrado S. (2003), Release of amoxicillin from polyionic complexes of Chitosan and poly(acrylic acid) study of polymer/polymer and polymer/drug interactions within the network structure. *Biomaterials*, 24, 1499-1506.

Uhlmann P, Houbenov, Stamm M, & Minko S. (2005) Surface functionalization by smart binary polymer brushes to tune physico-chemical characteristics at biointerfaces. *E-Polymers*, 75, 1–10.

Varum, K.M., Myhr, M.M., Hjerde, R.J.N., & Smidsrod, O. (1997). In vitro degradation rates of partially N-acetylated Chitosans in human serum. *Carbohydrate Research*, 299, 99–101.

Wang, T., Turhan, M., & Gunasekaran, S. (2004b). Selected properties of pH-sensitive, biodegradable chitosan-poly(vinyl alcohol) hydrogel. *Polymer International,* 53, 911–918.

Wang, D., Williams, C. G., Yang, F., & Elisseeff, J. H. (2004a). Enhancing the tissue- biomaterial interface: Tissue-initiated integration of biomaterials. *Advanced Functional Materials*, 14, 1152–1159.

Wang, J.W., & Hon, M.H. (2005). Preparation of Poly(ethylene glycol)/Chitosan Membranes by a Glucose-Mediating Process and *In Vitro* Drug Release. *Journal of Applied Polymer Science,* 96, 1083–1094.

Ward, A. M. & Georgiou, T. K. (2011). Thermoresponsive polymers for biomedical applications. *Polymers*, 3, 1215-1242.

Wu, J. Y., Liu S.Q., Heng, P.W.S., & Yang, Y.Y. (2005). Evaluating proteins release from, and their interactions with, thermosensitive poly (N-isopropylacrylamide) hydrogels. *Journal of Controlled Release* 102, 361-372.

Xing, Y. L., Xiang, Y. K., Shuai, S., Ying, C. G., Li, Y., Gang, G., Feng, L., Xia, Z., Yu, Q. W., Zhi, Y. Q. (2010) Biodegradable MPEG-g-Chitosan and methoxy poly(ethylene glycol)-β-poly(ε-caprolactone) composite films: Part 1. Preparation and characterization. *Carbohydrate Polymers* 79 429–436.

Xu, F, Kang, E, & Neoh, K. (2006). pH- and temperature-responsive hydrogels from crosslinked triblock copolymers prepared via consecutive atom transfer radical polymerizations. *Biomaterials,* 27, 2787–2797.

Yadav, K. S., Satish, C. S. & Shivakumar, H.G. (2007). Preparation and evaluation of Chitosan-poly (acrylic acid) hydrogels as stomach specific delivery for amoxicillin and metronidazole. *Indian Journal of Pharmaceutical Sciences.* 69, 91-95.

Yong, W.C., Sung, S.H., Sohk, W.K. (2000). PVA containing chito-oligosaccharide side chain. *Polymer*, 41, 2033–2039.

Zhang, R., Tang, M., Bowyer, A., Eisenthal, R., & Hubble, J. (2005). A novel pH and ionic strength-sensitive carboxymethyl dextran hydrogel. *Biomaterials,* 26, 4677–4683.

Zhang, X.Z., Lewis, P.J., & Chu, C.C. (2005). Fabrication and characterization of a smart drug delivery system: microspheres in hydrogel. *Biomaterials*, 26, 3299–3309.

Zhang, X.Z., Yang, Y.Y., Chung, T.S., & Ma, K.X. (2001). Fabrication and characterization of vast response poly(N-isopropyl acrylamide) hydrogels. *Langmuir*, 17, 6094–6099.

Zhu, A., Chen, T., Yuan, L., Wu, H. & Lu, P. (2006). Synthesis and characterization of N-succinyl-Chitosan and its self-assembly of nanospheres. *Carbohydrate Polymers*, 66, 274–279.